University of Windsor

Scholarship at UWindsor

Electronic Theses and Dissertations

Theses, Dissertations, and Major Papers

2010

Development of Hybrid Mg-based Composites

Zhang Qiang
University of Windsor

Follow this and additional works at: https://scholar.uwindsor.ca/etd

Development of Hybrid Mg-based Composites

By

Qiang Zhang

A Thesis

Submitted to the Faculty of Graduate Studies and Research

through Engineering Materials

in Partial Fulfillment of the Requirements for

the Degree of Master of Applied Science

at the University of Windsor

Windsor, Ontario, Canada

2009

Development of Hybrid Mg-based Composites

By

Qiang Zhang

APPROVED BY

_____

C. Chen, Outside Program Reader
Electrical Engineering Graduate program

_____

D. Green, Program Reader
Engineering Materials Graduate program

_____

H. Hu, Advisor
Engineering Materials Graduate program

_____

R. Bowers, Chair of Defense
Engineering Materials Graduate program

AUTHOR'S DECLARATION OF ORIGINALITY

I hereby certify that I am the sole author of this thesis and that no part of this thesis has been published or submitted for publication.

I certify that, to the best of my knowledge, my thesis does not infringe upon anyone's copyright nor violate any proprietary rights and that any ideas, techniques, quotations, or any other material from the work of other people included in my thesis, published or otherwise, are fully acknowledged in accordance with the standard referencing practices. Furthermore, to the extent that I have included copyrighted material that surpasses the bounds of fair dealing within the meaning of the Canada Copyright Act, I certify that I have obtained a written permission from the copyright owner(s) to include such material(s) in my thesis and have include copies of such copyright clearances to my appendix.

I declare that this is a true copy of my thesis, including any final revisions, as approved by my thesis committee and the Graduate Studies office, and that this thesis has not been submitted for a higher degree to any other University or Institution.

ABSTRACT

Metal matrix composites have widely been recognized to possess superior mechanical properties at both room and elevated temperatures, such as high elastic modulus and strengths as well as enhanced wear resistance, compared to the unreinforced monolithic metal. In this study, a novel approach of making hybrid preforms with two or more types of reinforcements, i.e., low-cost and different sized particles and fibres, for magnesium-based composites was developed. An advanced and affordable technique of fabricating hybrid magnesium based composites named the preform-squeeze casting was employed successfully. The microstructural analyses show that both the particles and fibres distribute homogeneously in the preform and its matrix materials of the composites. The grain refinement mechanisms of the hybrid composites during solidification were investigated. The engineering performance of the composites was evaluated by tensile testing in comparison with the matrix alloy. The tensile testing results indicate that the tensile properties of the hybrid composites with ($4\text{vol}\%\,Al_2O_3$ particles + $9\text{vol}\%\,Al_2O_3$ fibres) are considerably improved over those of the matrix magnesium alloy.

DEDICATION

I dedicate this thesis to my wife, my daughter and my near future son, who will be born in December, 2009. Their love, support, encouragement and patience during my study at the University of Windsor has given me the strength, and enable me to go through the difficult time during the research period, and finally complete this work.

ACKNOWLEDGMENTS

I would like to express my appreciation to my supervisor Dr. Henry Hu, for giving me this great opportunity to study in the engineering materials program of the University of Windsor, and for his kindly suggestion, encouragement and excellent supervision of this research work.

Great thanks to Dr. Green and Dr. Chen for taking the time for my proposal and research presentations, as well reviewing my thesis and giving me suggestions for this project.

I am very grateful to Mr. Andy Jenner, Mr. Steve Budinsky and other technicians of the Technical Support Center, Mr. Patrick F. Seguin and Mr. John Robinson for their technical assistance in the experimental analysis and tests in this research, and also to classmates in my group: LiHong Han, Zhizhong Sun, and Jonathan R.Burns, for their informative and valuable discussion.

Most of all I would like to express my deepest gratitude to my family: my wife, my daughter and my future son for their love, understanding, encouragement and support.

CONTENTS

CHAPTER 3

EXPERIMENTAL PROCEDURE

CHAPTER 4

RESULTS AND DISCUSSION

LIST OF FIGURES

LIST OF TABLES

CHAPTER 1

INTRODUCTION

1.1 Background

The need for high-performance and lightweight materials in the automotive and aerospace industries has led to extensive research and development efforts in the development of magnesium matrix composites and their cost-effective fabrication technologies. Composite materials are versatile in terms of constituent selection so that the properties of the materials can be tailored. The major disadvantage of metal matrix composites usually lies in the relatively high cost of fabrication and of the reinforcement materials. The cost-effective processing of composite materials is, therefore, an essential element for expanding their applications. The availability of a wide variety of reinforcing techniques is attracting interest in composite materials. This is especially true for the high performance magnesium materials due to certain unique characteristics of composites which offer effective approaches to strengthen magnesium alloys.

Hybrid composites are fabricated by adding two or more reinforcements into matrix materials so that excellent properties can be achieved through the combined advantages of short fibres, and different size particles, which provide a high degree of design freedom. Hybrid metal matrix composites are reinforced with hybrid reinforcement in which both particles and short fibres are employed. As a result, they can provide large opportunities to optimize the engineering performance of metal matrix composites for potential applications in the automotive and aerospace industries, where different volumes, especially the relatively low volume, and selective reinforced areas of reinforcements are required.

The hybrid metal-based composites could be fabricated by preform-squeeze casting, in which a two-step process is involved. First, a preform is made and then the squeeze casting pressurizes molten alloy to infiltrate into the preform. The advantages of preform-squeeze cast hybrid composites are the following: both the particles and short fibres can be employed to facilitate microstructure design and mechanical property optimization; reasonable low cost raw materials and wide volume percentage range of reinforcements can be selected; mass production becomes feasible; and improvements in the wettability of reinforcements enable selected regions of parts to be reinforced only with no wetting agent.

However, in the open literature, there are few studies on hybrid magnesium-based composites which are fabricated by the preform-squeeze casting technique. No detailed research reports on processing, solidification and characterization of hybrid magnesium-based composites have been found.

1.2 Objectives of this study

The objectives of this work are outlined as follows:

- Develop a process for preform fabrication;

- Develop a process for manufacturing hybrid magnesium-based composites;

- Investigate the characteristics of the developed preforms;

- Study the solidification behavior of the hybrid magnesium-based composites;

- Analyze the microstructure evolution of the developed hybrid magnesium-based composites; and

- Evaluate the mechanical properties of the hybrid composites.

1.3 Organization of the thesis

This thesis contains six chapters. Chapter 1 provides a general background of metal-based composites and the advantages of hybrid metal matrix composites fabricated by preform-squeeze casting technique. Chapter 2 reviews recent studies on the processing, microstructure, and mechanical properties of magnesium-matrix composites. The experimental procedures and the employed process used in this work are described in chapter 3. Chapter 4 reports the detailed results and discussion with respect to the effects of hybrid reinforcement including both particles and fibres contents on microstructure and solidification and tensile properties of the developed hybrid magnesium-based composites. The conclusions of the present study are summarized in Chapter 5. Finally, Chapter 6 gives some recommendations for future work.

CHAPTER 2

LITERATURE REVIEW

Magnesium alloys have been increasingly used in the automotive industry in recent years due to their lightweight. The density of magnesium is approximately two thirds of that of aluminum, one quarter of zinc, and one fifth of steel. As a result, magnesium alloys offer a very high specific strength among conventional engineering alloys. In addition, magnesium alloys possess good damping capacity, excellent cast ability, and superior machine ability. Accordingly, magnesium casting production has experienced an annual growth of between 10 and 20% over the past decades and is expected to continue at this rate [1-4]. However, compared to other structural metals, magnesium alloys have relatively low absolute strengths, especially at elevated temperatures. Currently, the most widely used magnesium alloys are based on the Mg-Al system. Their applications are usually limited to temperatures of up to 120°C. Further improvement in the high-temperature mechanical properties of magnesium alloys will greatly expand their industrial applications. In the past decades, efforts to develop high temperature magnesium materials have led to the development of several new alloy systems such as Mg-Al-Ca [5], Mg-Re-Zn-Zr [6], Mg-Sc-Mn [7] and Mg-Y-Re-Zr [8] alloys. However, this progress has not generated extensive applications of these magnesium alloys in the automotive industry, either because of insufficient high temperature strengths or high cost.

The need for high-performance and lightweight materials for some demanding applications has led to extensive R&D efforts in the development of magnesium matrix composites and cost-effective fabrication technologies. For instance, the magnesium matrix composite unidirectional reinforced with continuous carbon fibre can readily show a bending strength of 1000MPa with a

4

density as low as $1.8g/cm^3$. The superior mechanical property can be retained at elevated temperatures up to 350-400°C [9-11]. Moreover, composite materials are flexible in terms of constituent selection so that the properties of the materials can be tailored. The major disadvantage of metal matrix composites usually lies in the relatively high cost of fabrication and of the reinforcement materials. The cost-effective processing of composite materials is, therefore, an essential element for expanding their applications. The availability of a wide variety of reinforcing techniques is attracting interest in composite materials. This is especially true for high performance magnesium materials, since the characteristics of a composite provide an effective approach to strengthening magnesium alloys. Mg-Li binary alloys at around the eutectic composition, for example, are composed of HCP (α) and BCC (β) solid solution phases. The dissolution of Li into Mg causes a minor solution strengthening effect without the formation of any Mg-Li precipitates during the cooling process [12]. Thus, heat treatment based on phase transformation cannot be applied to improve their properties. Efforts to strengthen this binary system by producing LiX (X= Al, Zn, Cd etc.) type precipitates have not been successful because these precipitates tend to overage easily, even at room temperature [13-15]. In contrast, the incorporation of thermally stable reinforcements into composite materials makes them preferable for high temperature applications. The potential applications of magnesium matrix composites in the automotive industry include their use in: disk rotors, piston ring grooves, gears, gearbox bearings, connecting rods, and shift forks. The increasing demand for lightweight and high performance materials is likely to increase the need for magnesium matrix composites. This chapter reviews recent studies on the processing, microstructure, and mechanical properties of magnesium-matrix composites.

2.1 Processes for fabricating metal matrix composites

A key challenge in the processing of composites is to homogeneously distribute the reinforcement phases in the matrix to achieve a defect-free microstructure. Based on the shape, the reinforcing phases in the composite can be either particles or fibres. The relatively low material cost and suitability for automatic processing has made the particulate-reinforced composite preferable to the fibre-reinforced composite for automotive applications.

Due to the similar melting temperatures of magnesium and aluminum alloys, the processing of a magnesium matrix composite is very similar to that of aluminum matrix composites. For example, the reinforcing phases (powders/fibres/whiskers) in magnesium matrix composites are incorporated into a magnesium alloy mostly by conventional methods such as stir casting, squeeze casting, and powder metallurgy.

2.1.1 Stir casting

In a stir casting process, the reinforcing phases (usually in powder form) are distributed into molten magnesium by mechanical stirring. Stir casting of metal matrix composites was initiated in 1968, when S.Ray introduced alumina particles into aluminum melt by stirring molten aluminum alloys containing the ceramic powders. Figure 2-1 shows the typical stir casting process [16]. Mechanical stirring in the furnace is a key element of this process. The resultant molten alloy, with ceramic particles, can then be used for die casting, permanent mold casting, or sand casting. Stir casting is suitable for manufacturing composites with up to 30% volume fractions of reinforcement. The cast composites are sometimes further extruded to reduce porosity, refine the microstructure, and homogenize the distribution of the reinforcement. Magnesium composites with various matrix compositions, such as AZ31, Z6, CP-Mg

6

(chemically pure magnesium), ZC63, ZC71, and AZ91, have also been produced using this method [17-21].

(a)

(b)   (c)
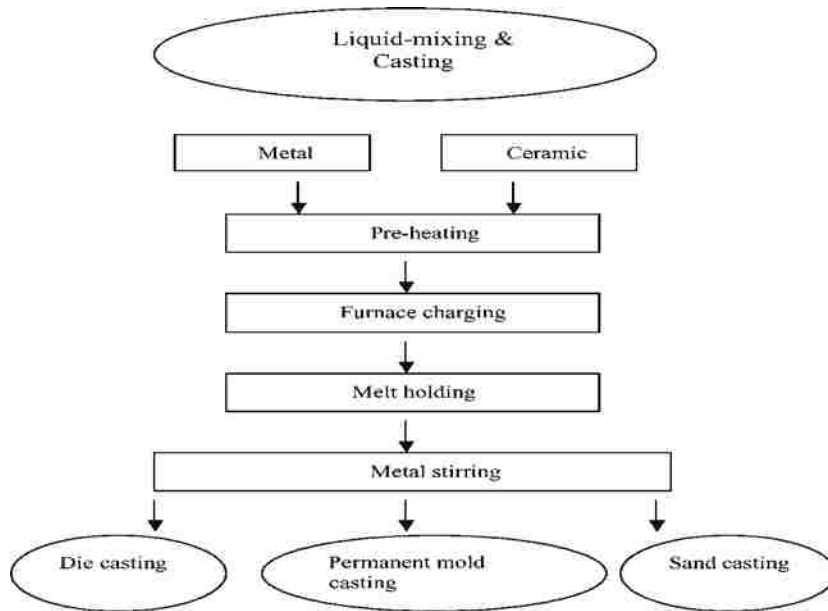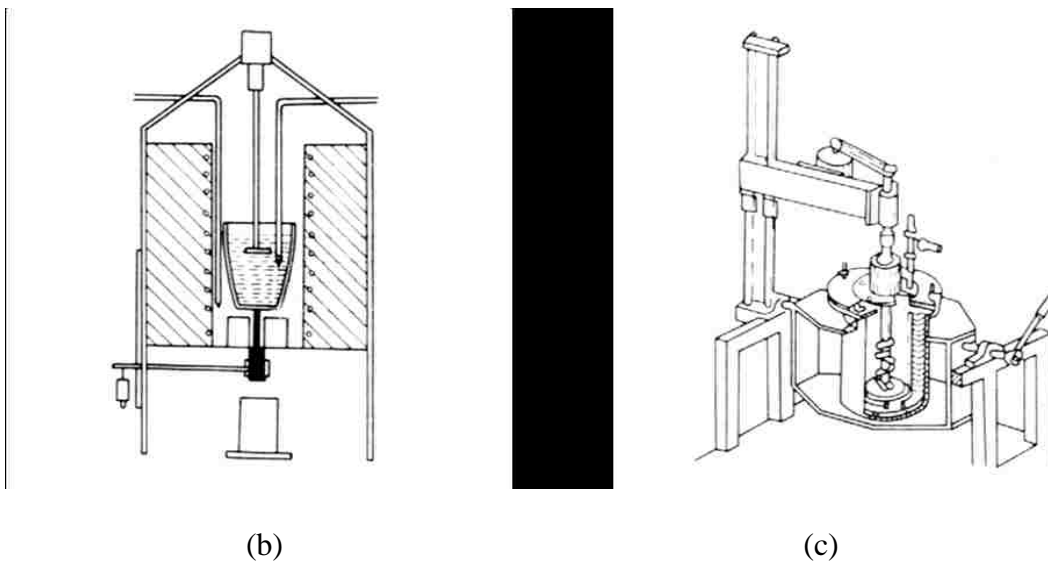
Figure 2-1 Typical stir casting process, (a) a process flow chart [16], (b) semisolid slurry casting [18] and (c) Duralcon casting [19].

A homogeneous distribution of secondary particles in the composite matrix is critical for achieving a high strengthening effect because an uneven distribution can lead to premature failures in both reinforcement-free and reinforcement-rich areas. The reinforcement-free areas tend to be weaker than the other areas. Under an applied stress, slip of dislocations and initiation of micro-cracks can occur in these areas relatively easily, eventually resulting in failure of the materials. In the areas of significant segregation or agglomeration of normally highly brittle hard particles, weak bonds are formed in the material which can lead to reduced mechanical properties.

A major concern associated with the stir casting process is the segregation of reinforcing particles which is caused by the surfacing or settling of the reinforcement particles during the melting and casting processes. The final distribution of the particles in the solid depends on material properties and process parameters such as the wetting condition of the particles with the melt, strength of mixing, relative density, and rate of solidification. Solidification of any melt-stirred composites will result in an uneven distribution of particles on a micro scale. This is caused by the 'pushing' phenomenon where the growing matrix dendrite expels the particles as it grows. The result is a necklace distribution of particles. The severity of this is thus dependent on grain size and can be minimized by using fine grained alloys or rapid cooling rate processed. The distribution of the particles in the molten matrix depends on the geometry of the mechanical stirrer, stirring parameters, placement of the mechanical stirrer in the melt, melting temperature, and the characteristics of the particles added.

An interesting recent development [22] in stir casting is a two-step mixing process. In this process, the matrix material is heated to above its liquids and solidus points and kept in a semi-solid state. At this stage, the preheated particles are added and mixed. The slurry is again heated

to a fully liquid state and mixed thoroughly. This two-step mixing process has been used in the fabrication of aluminum A356 and 6061 matrix composites reinforced with SiC particles. The resulting microstructure has been found to be more uniform than that processed with conventional stirring.

The effectiveness of this two-step processing method is mainly attributed to its ability to break the gas layer around the particle surface. Particles usually have a thin layer of gas absorbed on their surface, which impedes wetting between the particles and molten metals. Compared with conventional stirring, the mixing of the particles in the semi-solid state can more effectively break the gas layer because the high melt viscosity produces a more abrasive action on the particle surface. Hence, the breaking of the gas layer improvers the effectiveness of the subsequent mixing in a fully liquid state.

Another concern with the stir casting process is the entrapment of gases and unwanted inclusions. Magnesium alloy is sensitive to oxidation. Once gases and inclusions are entrapped, the increased viscosity of the vigorously stirred melt prevents easy removal of these detriments. Thus, the stirring process needs to be more judiciously controlled for a magnesium alloy than for an aluminum alloy in order to prevent the entrapment of gases and inclusions.

In principle, stir casting allows for the use of conventional metal processing methods with the addition of an appropriate stirring system such as mechanical stirring; ultrasonic or electromagnetic stirring; or centrifugal force stirring. The major merit of stir casting is its applicability to large quantity production. Among all the well-established metal matrix composite fabrication methods, stir casting is the most economical (Compared to other methods, stir casting costs as little as one third to one tenth for mass production). For that reason, stir casting is currently the most popular commercial method of producing aluminum based

composites. However, no commercial use of stir casting has been reported on magnesium matrix composites.

2.1.2 Squeeze casting

Although the concept of squeeze casting dates back to the 1800s, the first actual squeeze casting experiment was not conducted until 1931. Figure 2-2 illustrates the process of the squeeze casting of a magnesium matrix composite [2]. During squeeze casting, the reinforcement (either powders or fibres/whiskers) is usually made into a preform and placed into a casting mold. The molten magnesium alloy is then poured into the mold and solidified under high pressure. Compared with stir casting, squeeze casting has the advantages of allowing for the incorporation of higher volume fractions (up to 40-50%) of reinforcement into the magnesium alloys, and the selective reinforcement of a portion of a mechanical component. Numerous magnesium matrix composites such as SiCw/ Mg, SiCw/AZ91, Mg_2Si/Mg, have been produced using this technology [23, 24].
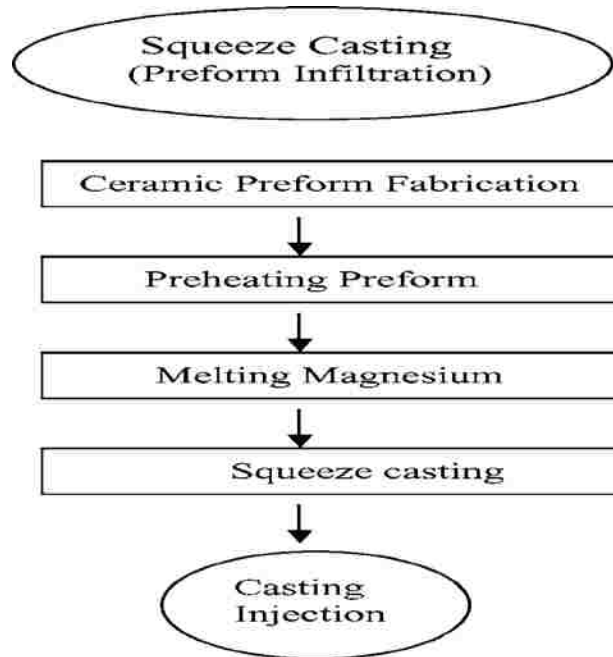
Figure 2-2 A process of perform squeezing casting [2].

The applied pressure is the primary variable which affects the microstructure and mechanical properties of the casting [25-27]. Under high pressure, several unique phenomena take place in the solidifying melt. The first is the shift of the freezing temperature. According to the Clausius-Clapeyron equation $dT/dP = T_f (V_s-V_l) / L_f$ (where T_f is the equilibrium freezing temperature of the material, V_s the specific volume of solid, V_l the specific volume of liquid, and L_f the latent heat of solidification), the solidifying temperature of an alloy depends on: the amount of pressure applied, the difference in its liquid and solid specific volumes, and solidification latent heat. It has been found that the eutectic temperature and composition of Al-Si alloy was changed from 660°C and 12.6% Si to 613°C and 17.4% Si respectively at 1300 MPa. The dt/dp of pure magnesium has been calculated to be 0.0647C/MPa [28]. The second effect of the high pressure is the increased cooling rate due to the enhanced heat transfer that results from the closer contact between the mold walls and the solidifying melt. A study on the effects of

11

pressure on the solidification of some eutectic alloys showed that the cooling rate increased from 11°C/s for permanent mold casting to 282°C/s for squeeze casting. The use of high pressure also introduces effective compensation for the solidification contraction. Under high pressure, the shrinkage in a solidifying ingot can be filled. The resulting material has finer grains and a higher density which lead to a greater strength and especially to an improved ductility of the castings. The ultimate tensile strength and hardness of a squeeze cast Mg-4.2% Zn-RE alloy were improved by 15 to 40% over those produced by permanent mold casting, and the tensile and hardness properties of the Mg-4.2%Zn-RE alloy reinforced with alumina fibres were increased by a factor of two when compared to the permanent by a factor of two when compared to the permanent mold cast alloy. The high pressure also eliminates risers and feeders needed in normal gravity casting and thus increases casting yield. At the same time, the inherent cast-ability of the alloy becomes less important under high pressure. In addition, squeeze casting is a near-shape process with little or no need for subsequent machining.

In the magnesium matrix composites, however, the pressure for squeeze casting has to be properly controlled because an excessively high pressure may produce a turbulent flow of molten magnesium, causing gas entrapment and magnesium oxidation. The excessively high pressure can also damage the reinforcement in a composite material and reduce the mechanical properties of the composites. Thus, a two-step squeeze casting, consisting of infiltration at low pressure and solidification at high pressure of the matrix alloy has been successfully performed to fabricate a SiCw/ZK51A magnesium matrix composite [29-31]. The shortcomings of the squeeze casting process lie mainly in the constraints on the processing imposed by the casting shape and its dimensions.

Recently, researchers have paid extra attention to hybrid preform-squeeze casting to fabricate the composites reinforced with hybrid reinforcement in which both of the particles and short fibres are employed [32, 33]. Hybrid composites are fabricated by adding two reinforcements into matrix materials so that the expected excellent properties can be achieved through the combined advantages of short fibres, and different size particles (micron or submicron), which provide a high degree of design freedom, and they provide large opportunities to optimize the engineering performance of the metal matrix composites for potential applications in the automobile industry, where relatively low volume of reinforcement is required. The advantages of hybrid composites are as follows:

- Both the particles and short fibres are employed to facilitate microstructure design and mechanical property optimization;

- Capability of mass production;

- Improvements in the wettability of reinforcement; and

- Ability to reinforce selected regions of parts only [31].

The comparison of the stir and squeeze casting processes for the fabrication of composites is summarized in Table 1-1.

Table 1-1 Comparison of squeeze casting to stir casting for composites

Melting Metallurgy Processes		Disadvantages	Advantages
Stir casting	Semisolid slurry casting	• Gas access into the melt • Reinforcements tend to form agglomerates • Unwanted porosities • Over reaction	• Low cost
	Duralcon casting	• High cost • Unstable distribution of reinforcement in matrix	• Mass production
Preform Squeeze Casting		• Squeezing equipment	• Reasonable costs • Selective reinforcement

2.1.3 Powder metallurgy

A variety of magnesium matrix composites have also been fabricated through powder metallurgy such as SiC/AZ91, TiO_2/AZ91, ZrO_2/AZ91, SiC/QE22, and B4C/AZ80 [32-36]. In the powder metallurgical process, magnesium and reinforcement powders are mixed, pressed, degassed and sintered at a certain temperature under a controlled atmosphere or in a vacuum. The advantages of this processing method include the capability of incorporating a relatively high volume fraction of reinforcement and fabrication of composites with matrix alloy and

reinforcement systems that are otherwise immiscible by liquid casting. However, this method requires alloy powders that are generally more expensive than bulk materials, and involves complicated processes during the material fabrication. Thus, powder metallurgy may not be an ideal processing technique for mass production. Figure 2-3 shows the typical powder metallurgical processes [34].

(a)   (b)   (c)   (d)
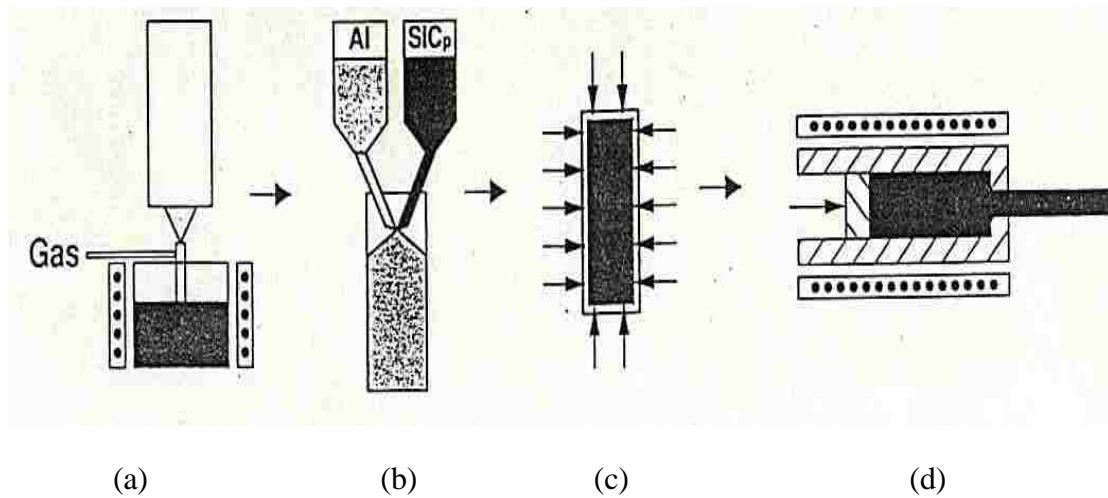
Figure 2-3 Typical powder metallurgical processes, (a) atomize alloy, (b) blend, (c) compact, and

(d) hot press and extrude [34].

The fabrication methods described above are well established and embody the mainstream of the manufacturing routes for magnesium matrix composites. A comparative evaluation of these traditional metal matrix composite processing techniques is provided in Table 2-2.

Table 2-2 Characteristic comparison of the melting and powder metallurgy processes

Processes	Densification	Anti-distortion	Wear resistance	Mechanical properties	Manufacturing costs
Melting (Stir and squeeze casting)	normal	good	good	good	low
Powder	good	bad	good	good	high

2.1.4 Summary

Based on the above discussion, it can be found that preform-based squeeze casting is an effective process to fabricate the metal matrix composites, and could be broadly used in automobile and aerospace industries. Table 2-3 shows the advantages and disadvantages of different types of preform-based composites.

Table 2-3 Advantages and disadvantages of different types of preform-based composites

Type	Disadvantages	Advantages
Short fibre reinforced preform-based composites	• Poor wear resistance	• Low cost • Selective reinforcement • Simple Process • Benefit for toughness
Particle reinforced preform-based composites	• Complex infiltration due to high particle density and fine pore diameters • At selective reinforcement extreme property step • Particle content 35-60% • High machining effort	• Low cost • Selective reinforcement
Hybrid (Fibre+Particle) preform-based composites	• Cost equipment	• Wide vol% range • Reasonable cost of reinforcements • Selective reinforcement

In fact, in most of practice cases, according to the working condition of components, high volume particle reinforcement is not necessary and it brings more disadvantages compared with low volume particle reinforcements. From Table 2-3, actually, in engineering cases the disadvantages of hybrid preform-squeeze casting in fabricating the composites would tolerances. As a result, the following conclusion would be summarized for hybrid composites:

Hybrid composites = two or more types reinforcements which are short fibres, and different size particles are added into matrix materials.

Advantages:

- Flexibility in microstructure design and mechanical property optimization;

- Capability of mass production;

- Improvements in the wettability of reinforcement; and

- Ability to reinforce selected regions of parts.

2.2 Microstructure of magnesium matrix composites

The key features in solidification of a composite material resulting from the interaction between the matrix and the reinforcement usually include the type, size, and distribution of secondary reinforcing phases, matrix grain size, matrix and secondary phase interfacial characteristics, and microstructure defects since the mechanical properties of the composite materials are strongly influenced by these factors. Figure 2-4 shows the typical microstructure of composites by stir casting [37]. Figure 2-5 shows the typical microstructure of composites by hybrid preform-squeeze casting [33].
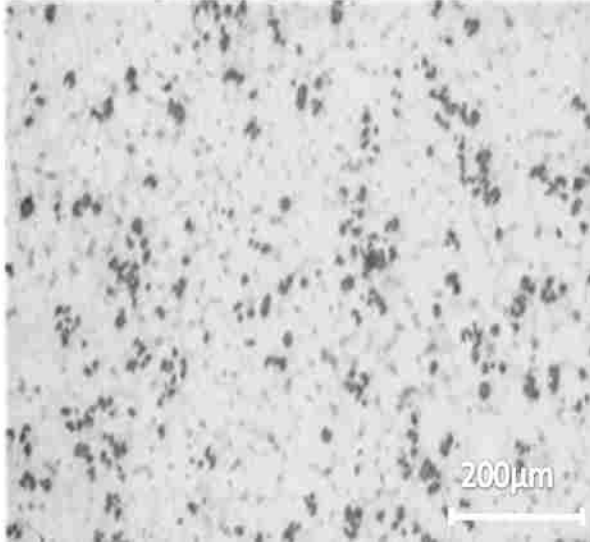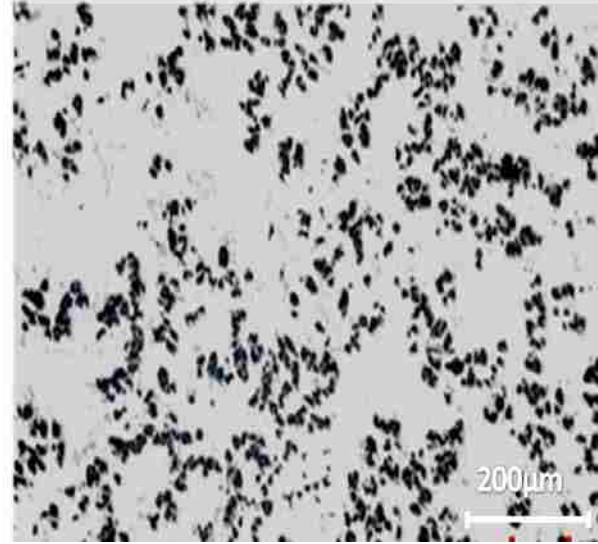
(a)	(b)

Figure 2-4 Typical microstructure of composites by stir casting, (a) 5vol.SiC/AM50 and (b) 10vol. %SiC/Al363 [37].
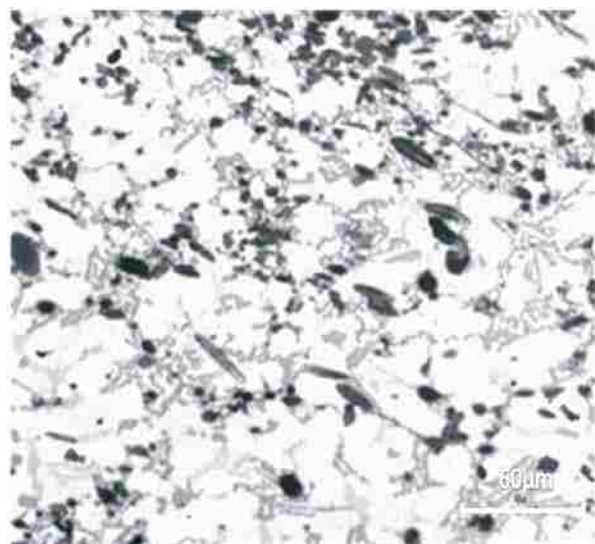
(a)	(b)

Figure 2-5 Typical microstructure of hybrid composite, (a) (5%vol. Al_2O_3particles+8%vol. Al_2O_3 fibres)/Al-Si and (b) (5vol. %Al_2O_3 particles +8 % vol.Al_2O_3 fibres)/AZ91 [33].

2.2.1 Reinforcement

Ceramic particles are the most widely studied reinforcement for magnesium matrix composites. Some common properties of ceramic materials make them desirable for reinforcements. These properties include low density and high levels of hardness, strength, elastic modulus, and thermal stability. However, they also have some common limitations such as low wettability, low ductility, and low compatibility with a magnesium matrix. Among the various ceramic, SiC is the most popular because of its relatively high wettability and its stability in magnesium melt, as compared to other ceramics.

The shape of reinforcement is another factor affecting the reinforcing effect. In a magnesium matrix composite, the most commonly used reinforcements assume a shape of short fibre/whisker, or particle, or a mixture of these two configurations. Short fibre/whisker reinforced magnesium alloys usually show better mechanical properties than the particle reinforced magnesium alloy with some degree of anisotropic behaviour. The strengthening effect depends on the characteristics of the strengthening mechanism. To overcome the barriers of relatively high cost and the anisotropic properties associated with fibre reinforcement, some recent efforts have been made to reduce the fibre cost by developing a new fibrous material and using hybrid reinforcements that incorporate particles into fibres. For instance, because the cost of aluminum borate whiskers is about only 10% of that of SiC whiskers [38], this material has been used recently and shows promise for commercial applications of the magnesium matrix composite. The size of the reinforcement used has ranged from nanometers to micrometers.

Because metallic solids will generally have a much better wettability with liquid metals than with ceramic powders, the reinforcing of a magnesium matrix with metallic/ intermetallic particulates has recently been examined. Elemental metal powders, such as Cu, Ni, and Ti

particulates with a diameter of a few micrometers, have been used as reinforcement agents in magnesium matrix composites because of their high melting points and very low solubility in magnesium. The advantages of the metallic reinforcements lie in their high ductility, high wettability and high compatibility with the matrix as compared with ceramics, and their great strength and elastic modulus as compared to the magnesium matrix. A major concern in the use of the elemental metallic powders is that their relatively high density could compromise the lightweight of the magnesium-based composites. The higher specific strengths that the metallic powder reinforced composites have shown as compared to the ceramic reinforced ones indicated that the density increase was compensated for by the increased reinforcing effect of the metallic powders [39- 42]. Since the high density of the metal powders can also cause mixing difficulties. The process has to be carefully designed and controlled to minimize the segregation of the reinforcements.

2.2.2 Matrix alloy

Various magnesium alloy systems have been used as the matrix for composites. Mg-Al alloys such as AM60 and AZ91 are presently the most prevalent magnesium alloys utilized in the automotive industry. They are also the most widely studied matrix for magnesium-based composites. Other magnesium materials, such as pure magnesium, Mg-Li alloy, and Mg-Ag-Re (QE22) alloys, have also been employed as a matrix material, although less frequently.

Grain refinement is a key principle in the strengthening of engineering alloys. The yield strength of a material normally varies proportionally with the reciprocal square root of its grain size, as depicted by the well known Hall-Petch equation: $\sigma = \sigma_o + Kd^{(-1/2)}$, where σ is the yield stress, σ_o the yield stress of a single crystal, K a constant, and d the grain size. The value of K

generally depends on the number of slip systems and is greater for HCP metals than for FCC and BCC metals [43]. Consequently, HCP metals exhibit higher strength sensitivity to the grain size. A study on the effects of grain size on the strength of magnesium alloy AZ91 and aluminum alloy 5083 indicates that the yield stress of the Mg alloy becomes greater when the grain size is smaller than 2.2 µm.

In a metal matrix composite, the secondary reinforcing phase can significantly influence the grain size of the matrix. Some studies reported significant grain refinement in the matrix in the SiC particle reinforced AZ91 magnesium alloys, as shown in Figure 2-6 [44]. The grain refinement effect has been attributed to heterogeneous nucleation of the primary magnesium phase on SiC particles and the restricted growth of magnesium crystals caused by the presence of rigid SiC particles. The heterogeneous nucleation mechanism is supported by the fact that the smaller the SiC particles, the finer the grains of the composite matrix. This is because more nucleation sites are provided.
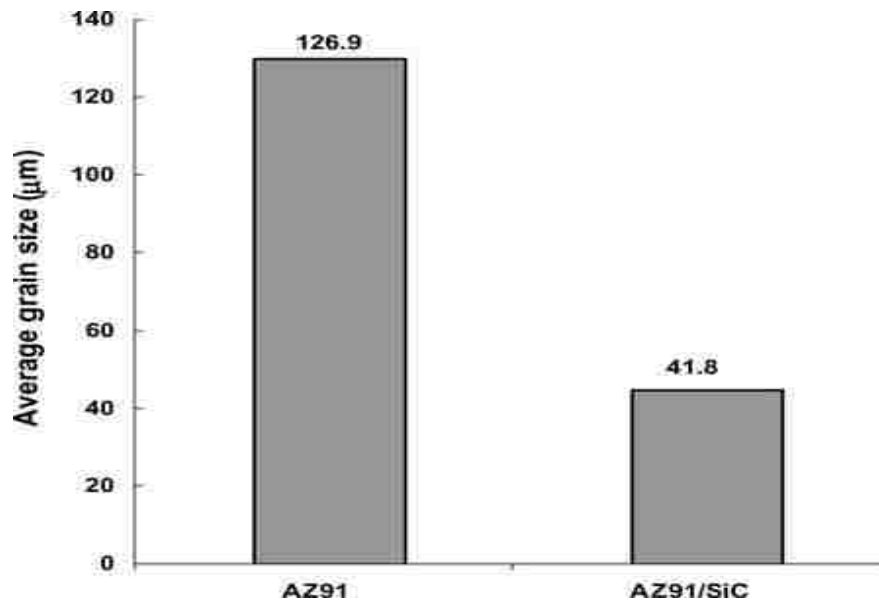
Figure 2-6 Grain size of AZ91 and SiC/AZ91 composites [44].

Fluid flow is of a completely different nature in fibre-reinforced metal solidification and, following nucleation, the matrix grains must grow. If (as is most often the case) nucleation was not initially on the reinforcement surface, the solid phase tends to avoid the reinforcement as it grows. The reinforcement acts as a barrier to solute diffusion ahead of the liquid/ solid interface and the growing solid phase will 'avoid' the reinforcement in much the same way that two growing dendrites avoid one another. Consequently, the last portion of the metal to solidify will be located close to or at the fibre/matrix, interface. This explains why, in the vast majority of fibre reinforced metals, the fibre/matrix interface is enriched in solute and in secondary phases.

On the other hand, it has also been reported [37] that the primary magnesium phase could not heterogeneously nucleate on the surface of SiC particles, and thus the SiC particles would not refine the matrix grains. Another study [45] on the microstructures of a metal matrix composite further suggests that the matrix grains may coarsen if no heterogeneous nucleation exists. That particular study reports that, whereas the liquid flow is an important condition to form fine grain microstructures in castings, the reinforcement hinders the convection of the liquid metal.

The conditions and mechanisms for heterogeneous nucleation of magnesium on the SiC particles were investigated in a recent paper [46]. The solidification microstructure of a 15vol% SiC/ Mg-Al-Zn composite that were investigated in the study showed that a majority of the SiC particles were pushed by the primary magnesium phases and segregated at the grain boundaries. At the same time, about 3% SiC particles were entrapped in the magnesium grain. The formation of the microstructure was discussed from the perspective of cooling, geometrical similarity, and surface defects of the SiC particles and the magnesium matrix.

In comparison to the ceramic particle reinforced magnesium matrix composite, the elemental metallic powder reinforced magnesium matrix composites are characterized by a

relatively uniform distribution of the metal particles. This enhanced homogeneity of the metal powder distribution results not only from the good wettability occurring between the reinforcing particles and the matrix, but also from the various engineering controls of the process such as a thin layered (sandwich) arrangement of raw materials when loaded in the crucible before melting, and the judicious selection of the stirring parameters.

2.2.3 Interfacial characteristics

The interface between the matrix and the secondary reinforcing phase plays a crucial role in the performance of composite materials. The key features of the interface are the chemical reactions and the strength of bonding. It was known that chemical reactions at the metal / reinforcement interface as well as to the necessity for the metal to break through its oxide layer to achieve intimate contact with the substrate.

Interfacial reactions in the magnesium matrix composite are predominately determined by the composition of the matrix and the reinforcement materials. A comparison study of the interfacial reactions in pure magnesium and AZ91 alloy based composites reinforced with SiC particles has evinced the effect of a matrix alloy composition on the particle/matrix interfacial phenomena. In the pure Mg based composite, SiC particles were stable and no reaction products were found at the interface. On the other hand, in AZ91 based composites the particle/matrix interfacial reactions were confirmed by the presence of an Mg_2Si phase. The involved reactions were $4Al+3SiC=Al_4C_3+3Si$ and then $Si + 2Mg= Mg_2Si$. Increasing the Al content in the alloy promoted the first reaction while increasing the Si content reduced the reaction [47]. Porosity also influences the interfacial reactions between the matrix and the reinforcing phases. For example, the reaction $3Mg+Al_2O_3=3MgO+2Al$, $2Mg+SiO_2=2MgO+Si$, in an AZ91 alloy

reinforced with 20vol% Al_2O_3 short fibres is not only influenced by the volume fraction of the fibres; but also by the fibre microstructure and porosity. Porosity might have increased the surface area and thus promoted the reaction.

The aluminum carbide reaction can be avoided by using high silicon alloys for the matrix, so for processing routes involving long contact times between the reinforcement and the melt, high silicon aluminum alloys are preferred. In powder processing using solid state consolidation, aluminum carbide formation is not a factor because silicon carbide is stable below the solidus; however, if liquid phase sintering is involved there is the potential for reaction. It is the molten metal processing routes that are particularly prone to reaction, since the particle-liquid metal contact times can be long, particularly when large scale casting processes, or remelting are involved. Other carbides, such as boron carbide and titanium carbide are also thermodynamically unstable in molten aluminum, but often react in a more complex manner.

Since magnesium has no stable carbide, ceramic carbides are stable in pure magnesium. However, many of the magnesium alloys of interest contain alloying elements, such as aluminum, which can form carbides, and in these magnesium alloys reaction may occur if the contact times are sufficiently long. Aluminum oxide, Al_2O_3, is stable in pure aluminums, but reacts with magnesium in Al-Mg alloys: $3Mg+Al_2O_3=3Mg+2Al$ and $3Mg+4Al_2O_3=3MgAl_2O_4+2Al$. At high magnesium levels, and lower temperatures, MgO may form, while the spinel will form down to very low magnesium levels. Al_2O_3 is not thermodynamically stable in most aluminum alloys. Other oxides, such as MgO, are expected to be stable. It should also be noted that, unlike SiC, which is stable below the solidus, this is not the case for Al_2O_3, and reaction can continue in the solid state. So solid state processing may still result in reinforcement reaction in this case. It was observed that the spinel crystals formed on the surface of Al_2O_3 particles after reaction above the

melting point in an Al-Mg alloy. Obviously, from above reaction equation, Al_2O_3 will be unstable to some extent in magnesium alloys, but other oxides, such as MgO and Y_2O_3 will be stable. However, in the case of preform-squeeze casting, the molten melt contacting with Al_2O_3 is in very short time (5-10 second). Since the molten melt is under higher pressure, it has higher cooling rate. The temperature of molten melt, such as magnesium alloy, will decrease to below solidus for solidification in 15-25 second. It was documented [25] that no heavy interface reaction can be observed. On the other hand, since the Al_2O_3 particles and fibres have lower cost compared with that of SiC, the combination of low-cost raw materials and effective process can match the requirement of automobile industry.

While these thermodynamic considerations show the tendency for reaction to occur, it is the kinetics and the extent of reaction which are of practical importance. There are three stages of the reaction which may be attributed to: first, nucleation of reaction product at preferred sites on the reinforcement; second, continued dissolution of reinforcement in direct contact with liquid aluminum; third, dissolution of the reinforcement separated from the liquid aluminum by reaction product and, in some cases, a solute enriched region.

The surface cleanliness of the raw materials is another factor affecting the interface chemical reactions. The reactions occurring in a squeeze cast AZ91 matrix composite with SiC fibres are $2Mg(l)+O_2(g) =2MgO(s)$ and /or $Mg(l) + O = MgO (s)$, where O_2 is produced from the absorption on the SiC fibre surface. The parameters of the casting process such as melting temperature and holding time have also been found to change the interface reactions in the magnesium matrix composite. Higher temperature normally accelerates interfacial reactions, as governed by the Arrhenius law. The degree of interfacial reactions can also change the microstructure. To obtain composite materials with the desired microstructure and properties, the

interfacial reaction should be controlled through selecting an appropriate matrix alloy, conducting an appropriate surface treatment of the reinforcement, and correctly controlling the process parameters.

The interface reactions in the SiC/QE22 composite are of particular interest. QE22 alloy has a good strength and creep resistance at elevated temperatures due to the formation of high melting point precipitates. However, unlike other magnesium matrix composites, the addition of SiC particles has been found to reduce the mechanical properties of the material [48]. This phenomenon has been attributed to the SiC and QE22 matrix interface features. The QE22 alloy has several types of precipitates such as Mg_3 (Ag, Nd), round a-Nd zone, rod-like Zr-Ni phase, MgO, and Mg-Nd GP zone. The every fine Mg-Nd GP zones play a key role in the precipitation hardening of the alloy. In the SiC/QE22 composite, all of the above-mentioned precipitates, except for the coherent GP zone, were observed. Furthermore, a pronounced precipitation of Nd-rich phase occurs at the SiC/matrix interfaces. Thus, the lack of GP zones in the composite may be attributed to the matrix depletion of Nd due to the precipitation of Nd-rich phases at the interfaces. This enhanced precipitation of Nd-rich phases at the SiC/ matrix interfaces can adversely affect the creep behaviour. Matrix depletion caused by the interfacial precipitation can produce inhomogeneous distribution of precipitates and a deficiency in the matrix precipitate microstructure, leading to composite weakening. Additionally, interfacial sliding may be another creep mechanism acting in the composite. As a result of interfacial sliding, many cavities can occur at the interfaces, giving rise to the macroscopic cracks and debonding of the matrix/SiC interfaces.

Interface reactions also take place in the elemental metallic powder reinforced magnesium matrix composite. In the composites with Cu and Ni reinforcement, reactions occur at the Mg/Cu

or Mg/Ni interfaces forming Mg_2Cu and Mg_2Ni intermetallic, respectively, leading to a reduction in the particle size of Cu and Ni powders. However, because of a higher wettability and compatibility, the matrix /reinforcement interface is free from such defects as debonding or microvoid.

2.2.4 Porosity and inclusions

Porosity and inclusions are detrimental to the mechanical properties in magnesium matrix composites and can remarkably reduce the creep resistance of the materials. At low porosity levels, the degree of damage to the mechanical properties caused by the porosity is the sum of that from each pore, in which case the tensile strength is found to be a linear function of the porosity density. This occurs because the distribution of the stress fields around each pore does not overlap. When the porosity volume fraction reaches a certain level, the stress fields of the pores overlap with each other, and the tensile strength of the materials is no longer linearly affected by the porosity [49].

The porosity in a composite may arise from a number of sources. These include: the entrapment of gases during mixing, hydrogen evolution, and the shrinkage of the alloy during its solidification. The entrapment of gases depends mainly on the processing method, such as mixing and pouring. Holding time and stirring speed as well as the size and position of the impeller can also significantly affect the porosity formation. The hydrogen production is mainly the result of the reactions between the absorbed H_2O and Mg melt. Usually some water vapour is absorbed on the surface of the added fibres or particles. Once entering the melt, the water vapour can react strongly with Mg, forming MgO and releasing H_2. Although gas porosity in casting is much more sensitive to the volume fraction of the inclusions than to the amount of dissolved H_2,

28

the recommended practice is to thoroughly dry the raw materials before adding them to the magnesium melt for the purposes of both safety and quality control. In the magnesium matrix composite, the presence of relatively large amounts of fibres/particles may impose a serious porosity problem if the reinforcement is not properly degassed prior to its addition to the melt. This is especially true for finer particles due to the larger number of specific surface areas involved.

Inclusions are another major microstructure defect that can reduce material properties. The inclusions normally encountered in magnesium alloys include magnesium oxide and nitride, Na, Ca, Mg, K-based chlorides, magnesium-based sulphide, fluoride, and sulphate. The processing of some metal matrix composites requires melt stirring. Some of the conventional methods for removing inclusions, such as flux refining and gas sparging and settling, may no longer be suitable for processing the metal matrix composites. Due to the high oxidation potential of the magnesium and the limitations of the oxidation protection, the inclusion content in cast magnesium alloys in usually 10-20 times higher than that in aluminum alloys [50]. In addition to the inclusion density, the inclusion size is also important in determining the mechanical properties of the composite materials. It was observed that larger inclusions are normally more harmful to the material's properties. Thus, care must be taken to prevent the formation of inclusions in the magnesium matrix composites.

2.3 Mechanical properties

2.3.1   Tensile strengths and elastic modulus

With the addition of a reinforcement phase, both the tensile strength and Young's modulus of magnesium alloys are, in general, increased. Within a certain range, both the yield strength

and the elastic modulus of the magnesium matrix composites increase linearly with the increase in volume fraction of the composite reinforcement. Hybrid reinforcements, which involve more than one kind of particle or whisker, have an even greater strengthening effect than a single reinforcement [51].

Particle strengthening, work hardening, load transfer, and grain refinement of the matrix alloy by the reinforcement phases are the key strengthening mechanisms in magnesium composites. The dispersion of fine and hard particles in the matrix drastically blocks the motion of dislocations and thus strengthens the material. Work hardening takes place when the composite is strained. The strain mismatch between the matrix and the reinforcement usually generates a higher density of dislocations in the matrix around the reinforcement, thus strengthening the material. Load transfer is a very important strengthening mechanism, especially for the fibre-reinforced composites. If the bonding between the matrix and the reinforcement is strong enough, the applied stress can be transferred from the soft matrix to the hard fibre/particle phases due to the much higher strength is highly sensitive to its grain size. Thus, grain refinement contributes to the great strength at room temperature for both Mg alloys and the Mg matrix composite. However, it was also reported that at typical volume fractions, Orowan strengthening is not a major factor with the 5μm and larger particles usually used, but particles of this size can result in quench hardening and enhanced work hardening because of elastic misfit back stress hardening. From these considerations, the strength of particle reinforced composites is most strongly dependent on the volume fraction of reinforcement with a somewhat weaker dependence on particle size.

Under an applied load, the stress built up in the magnesium composite can be relaxed by the cracking of the reinforcement. In a fractured SiC/Mg composite, the SiC particulate fracture

was observed to be the predominant form of localized damage under tensile loading. The fracture of the composite was dominated by the cracking of the reinforcing particulates that were present in the magnesium alloy metal matrix. Final fracture occurred as a result of crack propagation through the alloy matrix between particulate clusters. The size of the ceramic reinforcing particles is important here. In an investigation of the influence of SiC size and volume fraction on the mechanical properties of AZ91D, the addition of 15 µm SiC particles was found to increase fatigue resistance while the addition of 52 µm SiC particles reduced fatigue resistance due to the high brittleness of SiC. This difference depends on the extent to which the matrix and the reinforcement can deform cooperatively. A finer secondary phase can produce a more cooperated deformation within the matrix. In a 10 vol% SiC/ MB2 magnesium matrix composite, it has been found that after a high strain deformation, the matrix around small SiC particles (2 µm) had a fine grain microstructure and a strong bonding with these particles. In contrast, cavities were produced around the big SiC particles (5 µm). This is because the stress built up around the small particles can be more easily relaxed by cooperative deformation during the tensile test. Another advantage of the finer secondary phase is that it offers more heterogeneous nucleation sites for the solidification of the matrix magnesium alloy, which leads to a finer matrix grain size. Research results [52] have shown that the strength of a magnesium matrix composite does not monotonically increase with decreasing particle size, as the particle strengthening relies greatly on the stress built up around the particles by lattice distortion.

The stress built up in the metal matrix composite may also be relaxed by debonding along the reinforcement / matrix interfaces. In particular, when the matrix and reinforcement interface is a relatively weak region of the material, the composite may fail prematurely at the interfaces [53]. In this case, the addition of any secondary hard phase actually can reduce the material's

strength. Research focusing on an AZ91 magnesium alloy reinforced with 15 vol% SiC, TiB$_2$, TiC, Tin, AlN and Al$_2$O$_3$ has detected such an occurrence with AlN reinforcement [54]. This research also shows that the decrease in the tensile strength of AZ91, which has been attributed to excessive chemical reactions, different powder size distribution and wetting conditions, was caused by the addition of AlN.

The relative strengths of the matrix and interfaces can also be temperature dependent. The tensile behaviours of an AZ91 matrix composite reinforced with randomly oriented short carbon fibres showed that the failure mode of the composite changed from fibre/ MgO interface dominated failure to failure at the MgO/ matrix interface when the testing temperature is increased from room temperature to 200°C or higher [55].

In contrast to the composites reinforced with brittle ceramic hard phases, premature fractures of the reinforcement are not encountered in the elemental metallic powder-reinforced magnesium matrix composites. The high compatibility between the thermal and the mechanical properties and the good wettability between the matrix alloys and the secondary phase apparently leads to a highly cooperated deformation and a strong interface between the composite matrix and its reinforcement. As a result, the crack initiation in such composites, which originates from the matrix rather than from the secondary phase and interface, is noticeably delayed. The high toughness of the material is particularly advantageous when the applied load is impacted and large. Therefore, the introduction of strong and stiff high melting point metallic reinforcements in both pure magnesium and commercial grade magnesium alloys will significantly improve the overall mechanical properties, especially the strength and specific strength of the material.

Crack initiation and propagation in the reinforcement-free areas in the matrix are often observed in composite materials. In this case, the matrix plays a more important role in

determining the deformation and fracture behaviour of the composites. A comparison between pure magnesium and AZ91 reinforced with 10-20 vol %of Al_2O_3 fibres has evinced that the AZ91 matrix composite always exhibited a higher tensile yield strength, but the degree of strength improvement was greater in a pure magnesium composite. This phenomenon has been ascribed to the higher mechanical properties of AZ91 in comparison to pure magnesium. Accordingly, processes that modify the matrix microstructure can affect the mechanical properties of the bulk composite. Indications are that the thermal cycling of a SiCw/ZK60 magnesium matrix composite may first recover and age the matrix and then degrade the tensile properties of the material [56-61].

2.3.2 Ductility

The hard secondary phases in magnesium matrix composites have a two-fold effect. First, when these phases are present in magnesium matrix composites they can reduce their ductility by preventing plastic deformation. On the other hand, the particles can produce a grain refining effect that improves ductility. The net effect of the hard particles is, in general, to reduce ductility. This happens in both particle-reinforced and fibre-reinforced composites. In contrast with the ceramic reinforced magnesium matrix composites, the elemental metallic powder-reinforced magnesium matrix composites show a much better ductility because of the reduced possibility of breaking the particles and interface bond.

The reduced ductility in composites with a hard secondary phase is also evident in the interactions between the reinforcement and dislocations. It is obvious that the resistance to the dislocation motion of the hard particles reduces the ductility of the composite materials. A research study examining the super-plastic behaviour of fine-grained (~ 2 μm) WE43 magnesium

33

alloy containing spherical precipitates (~200 nm) within grains revealed a super-plasticity with an elongation-to failure of over 1000 percent at 400°C. Dislocations were observed to interact with the particles within the grains. Data analysis based on the constitutive equation for super-plastic flow demonstrated that the normalized strain rate for a particle-strengthened WE43 alloy was about 50 times lower than that of the same WE43 magnesium alloy without the hard precipitates. It would seem that the existence of intragranular particles diminishes the super-plastic flow. However, when compared to the breaking of large brittle particles and weak interface, the influence of very fine precipitates on the ductility may be less of a factor in magnesium matrix composite.

However, the high brittleness of secondary particles does not necessarily mean that a composite with hard phases will always have a low ductility. In fact, grain refinement by the secondary phase can result in super-plasticity in a magnesium matrix composite, even with highly brittle secondary phases. For example, a ZK60A magnesium alloy reinforced with 17 vol% of SiC particles showed a total creep elongation of 200-350% at the temperature range of 350-500°C. Another study has revealed a low temperature super-plasticity with an elongation to failure of 300% for the same material at 175-202°C due to the refined grains (about 1.7μm) [62]. This low-temperature super-plasticity is of significance for practical industrial applications of the magnesium matrix composite.

The secondary particles not only refine grains during the solidification process of the composite materials by providing heterogeneous nucleation sites, but also they retard the grain growth during mechanical processing and deformation processes at high temperatures. The composite was initially extruded to obtain a fine microstructure in the matrix with an average grain size of around 0.5 µm. At elevated temperatures, the grains in alloys tend to coarsen.

However, with the presence of fine hard particles, the growth of matrix alloy grains is obstructed, and the fine structure is retained at higher temperatures. There is a large amount of grain glide in such a fine microstructure, which contributes to its superplasticity. The role of the hard particles (also refined by the extrusion) in the composite is simply to impede grain growth and help to maintain the superplasticity. A uniform distribution of the hard particles in the matrix is a precondition for such a function. Although grain refinement can improve the strength and ductility at room temperature, it may accelerate creep deformation at elevated temperatures. Fine hard particles may improve the strength of magnesium alloys and also stabilize the grains at high temperatures, allowing for grain boundary sliding. Compared to aluminum matrix composites, it may be more difficult to attain high creep resistance for magnesium matrix composites because of the higher grain boundary diffusion rate in magnesium. However, it is still possible that a combination of excellent strength, ductility, and creep resistance can be realized, along with the addition of secondary hard phases.

2.3   Summary

Various techniques have been developed and applied to the processing of magnesium matrix composites, such as stir casting, pressure infiltration, and powder metallurgy. Key factors affecting the performance of the magnesium composites are the matrix composition; the chemistry; the shape, size, and distribution of the reinforcement; and the bonding strength at the reinforcement/matrix interface in the composites is normally achieved at the cost of compromised ductility. Nevertheless, grain refinement is an effective way of improving ductility and strength at ambient temperatures. However, caution has to be taken in using fine-grained materials at elevated temperatures because creep resistance can be adversely affected by the fine

grain size. The acceptance of magnesium matrix composites as engineering materials depends not only on the performance advantages of the materials, but also on the development of cost-effective processing technologies for these materials.

CHAPTER 3

EXPERIMENTAL PROCEDURE

3.1 Materials

Al$_2$O$_3$ ceramic particles and Al$_2$O$_3$ short fibres were employed as the raw materials for preparation of the hybrid reinforcements since they are relatively inexpensive and possess adequate properties. The matrix alloy was magnesium alloy AM60 with the chemistry composition (wt.%) of 6.0Al-0.22Zn-0.4Mn-0.1Si-0.01Cu-0.004Fe-0.002Ni-Mg due to its wide usage in the automotive industry and high ductility. The thermophysical properties of the ceramic Al$_2$O$_3$ particle and fibre as well as the matrix alloy (AM60) are shown in Table 3-1.

Table 3-1 Thermoplysical properties of property of ceramic Al$_2$O$_3$ particle and fibre [63-65]

Material	Al$_2$O$_3$ particle	Al$_2$O$_3$ fibre	AM60
Elasticity modulus / GN.m-2	380-450	200	35-44
Density /g.cm³	3.96	3.3~3.5	1.74
Diameter / μm (average)	3	4.0	
Heat expansion coefficient /10-6k-1	7.6	6	45
Specific heat / J.(kg.k) -1	1050	1000	1250
Thermal conductivity / W.(m.k)-1	7.5	5	85

3.2 Casting

A 75-ton, vertical hydraulic press as shown in Figure 3-1 was employed for squeeze casting hybrid composites. The melting was performed in an electrical resistance furnace. Figure 3-2 shows the electrical furnace with a control unit and a protective gas system.

Figure 3-1 Squeeze casting machine.   Figure 3-2 Melting unit.

Melting the pure magnesium or magnesium alloys requires the use of a protective gas mixture to protect the melt from oxidation and burning. The gas mixture employed in this study was the Sulfur Hexafluoride SF_6 0.5% plus carbon dioxide in balance. Since SF_6 density is far higher than air and oxygen, it can cover the top of the melt and separate the magnesium melt from air to prevent oxidizing. The flow rate of SF_6 mixed gas was controlled at 0.8 to 1.0 liter per minute with the outlet pressure of 20 to 25 psi during melting of magnesium alloys.

When running a squeeze casting experiment, a list of safety procedures and sequence must be followed at all time:

1. Do not use water when running an experiment;

2. Ventilation system is on;

3. Protection gas is on;

4. Safety hard hat with a full face shield, safety shoes, lab coat and leather gloves should be worn all the time;

5. Moulds and tools need to be preheated; and

6. Fire extinguisher can be quickly and easily accessed;

3.3 Fabrication of hybrid Preform

Figure 3-3 presents the flow chart of the process for fabricating hybrid preforms. The fabrication steps involve mixing of ceramic short fibers and particles, introduction of binding compounds, shape formation of preforms under pressure, drying and sintering. In the hybrid preform, the fibres serve as the cellular structure skeleton, and the content level of the fibre was pre-determined based on the desired amount of porosity levels of the cellular solid. Meanwhile, the particles were dispersed in the pores present in the cellular solid. The content, size and type of the ceramic reinforcements were adjusted with the definite quantity, and the shape of preforms. In addition, for the purpose of a comparative study of the characteristic of hybrid preform, the pure fibre preform was also fabricated using the same process without adding particle reinforcement.

In this study, the porosity of a hybrid preform is defined by the following equation [13]:

$$\rho_f = 1 - (\rho^*/\rho_s) \qquad\qquad\qquad \text{(Eq. 3-1)}$$

where ρ_f is porosity of the preforms, ρ^* is the density of the preform(*), and ρ_s is the density of the structure material (s) of the preform. Under the unit volume, the ρ_s can be calculated by the qualities of structure materials.
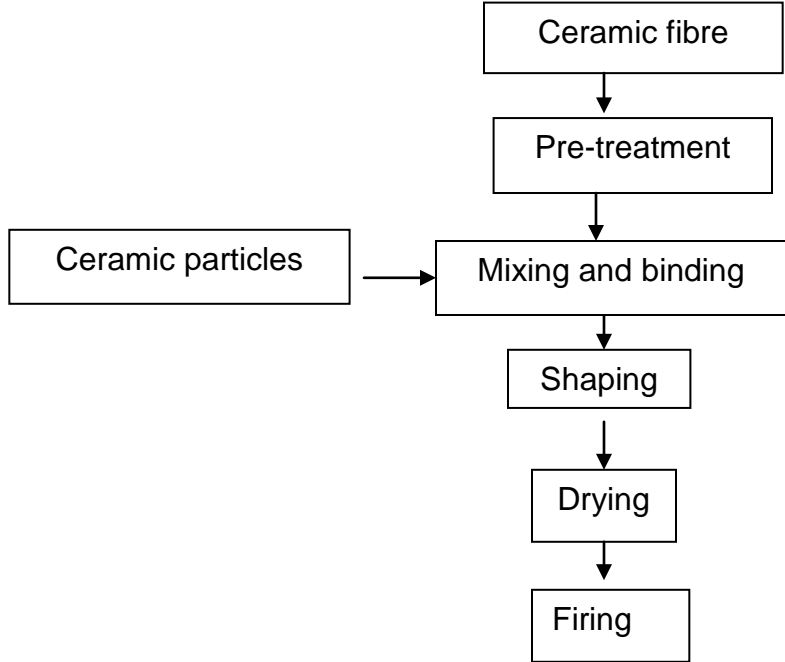
```
                    ┌─────────────────┐
                    │  Ceramic fibre  │
                    └─────────────────┘
                             │
                             ▼
                    ┌─────────────────┐
                    │  Pre-treatment  │
                    └─────────────────┘
                             │
                             ▼
┌──────────────────┐   ┌──────────────────────┐
│ Ceramic particles│──▶│  Mixing and binding  │
└──────────────────┘   └──────────────────────┘
                             │
                             ▼
                       ┌────────────┐
                       │  Shaping   │
                       └────────────┘
                             │
                             ▼
                       ┌────────────┐
                       │   Drying   │
                       └────────────┘
                             │
                             ▼
                       ┌────────────┐
                       │   Firing   │
                       └────────────┘
```

Figure 3-3 A flowchart showing the procedure for fabricating a hybrid preform.

3.4 Fabrication of composites

Figure 3-4 shows the fabrication process of the composites in which a squeeze casting process was adopted. During fabrication, a hybrid preform was first preheated to 300 $^{\circ}$C. Then, molten matrix alloy AM60 at 750 $^{\circ}$C infiltrated into the preheated preform under an applied pressure of 90 MPa. The pressure was maintained at the desired level for 25 seconds. After squeeze casting, a cylindrical disk of the dual-phase reinforced composite with 4 vol.% of Al_2O_3 particles and 9 vol.% of Al_2O_3 fibres, named (F+P)/AM60, was obtained. In the hybrid composite, the particles constituted the primary reinforcement phase, and short fibres served as the secondary reinforcement phase. For the purpose of comparison, a composite (F/AM60) with only 9vol. % of Al_2O_3 fibre reinforcement was also prepared but without particle addition.
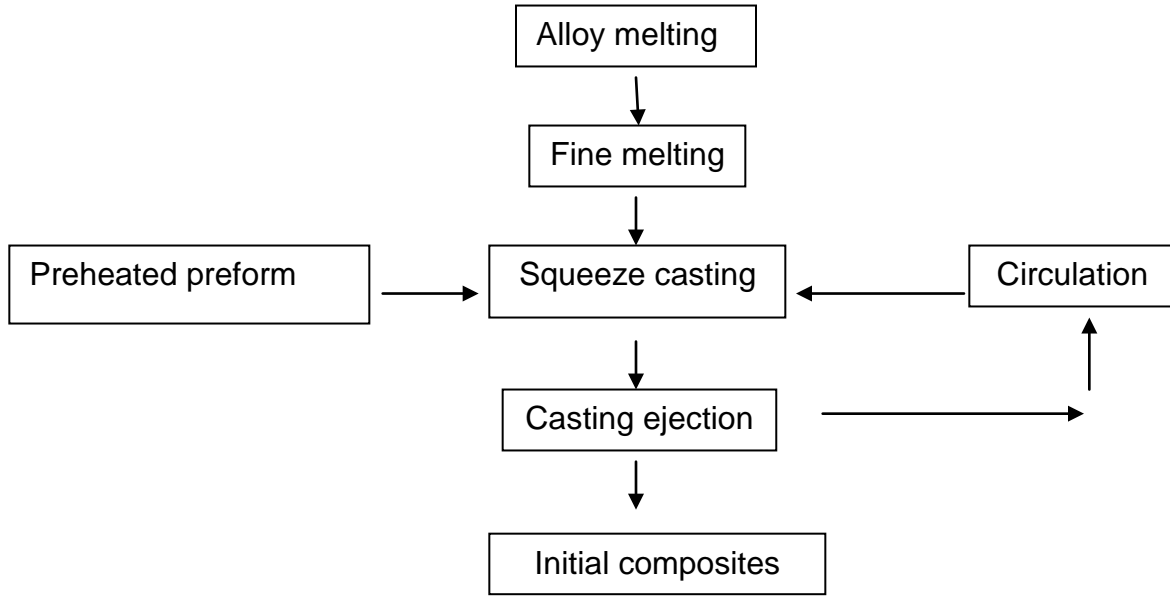
40

Figure 3-4 Flowchart showing the procedure for fabricating hybrid composites.

3.5 Tensile Testing

The mechanical properties of the matrix alloy and composites were evaluated by tensile testing, which was performed at ambient temperature on an Instron (Grove City, PA) machine equipped with a computer data acquisition system. Following ASTM B557, subsize flat tensile specimens (25 mm in gage length, 6mm in width, and 10 mm in as-cast thickness) were machined from the squeeze cast disks. The tensile properties, including 0.2% yield strength (YS), ultimate tensile strength (UTS), and elongation to failure (E_f), were obtained based on the average of three tests. Figure 3-5 is the schematic illustration of Tensile Test Specimen & machine.
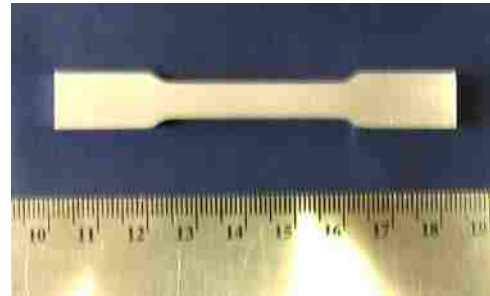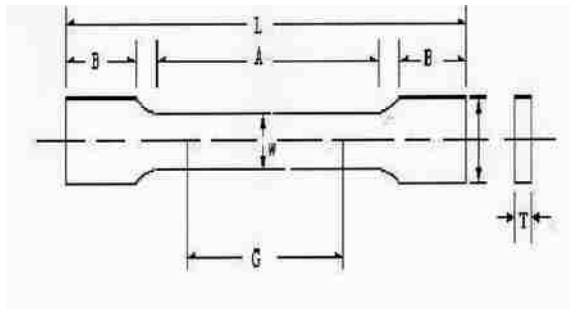
G-Gage length: 25±0.1mm   W-Width: 6±0.1mm

T-Thickness 6±0.1mm   R-Radius of fillet, min: 6mm

L-Overall length, min: 100 mm: A-Length of reduced section: 32mm

B-Length of grip section, min: 30 mm   C-Width of grip section: 10mm

Figure 3-5 Schematic illustration of Tensile Test Specimen & machine.

3.6 Hardness testing

Macrohardness measurements were conducted on the polished AM60 matrix alloy and composites. The Rockwell F scale was used for macrohardness measurement in accordance with ASTM E18-94 standard for both the matrix alloy and composites. Figure 3-6 the macrohardness testing equipment which is Wilson M1CI mode of Rockwell hardness tester.

Figure 3-6 Macrohardness testing equipment.

3.7 Microstructural analysis

Specimens were sectioned, mounted, and polished from the centre of the squeeze disk and prepared following the standard metallographic procedures. A Buehler (Lake Bluff, IL) optical image analyzer 2002 system shown in Figure 3-7 was used to determine the primary characteristics of the specimens. The detailed features of the microstructure were also characterized at high magnification using a JSM-5800LV (Tokyo, Japan) scanning electron microscope (SEM) with a maximum resolution of 100 nm in a backscattered model/l um in X-ray diffraction mapping mode, and maximum useful magnification of 30,000. Figure 3-8 shows the scanning electron microscope (JEOL Model JSM-5800 LV). In order to maximize the composition reading of the energy dispersive spectroscopy (EDS) data an etchant was applied to the polished specimens for microscopic examination. Fracture surfaces of tensile specimens were analyzed with the SEM to ascertain the nature of fracture mechanisms.
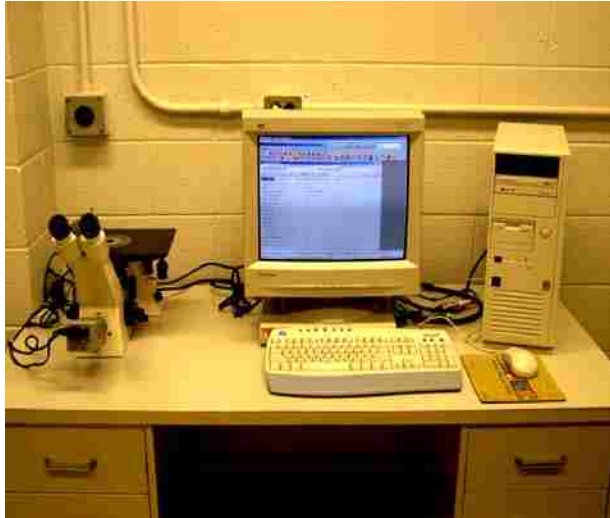
Figure 3-7 Buehler optical image   Figure 3-8 Scanning electron microscope

analyzer model 2002.   (JEOL Model JSM-5800 LV).

3.8 DSC analysis

The thermal analysis was carried out using a Differential Scanning Calorimetry-Thermogravimetric Analyzer (DSC-TGA Q600) manufactured by TA Instrument, as shown in Figure 3-9.

Figure 3-9 A differential scanning calorimetry-thermogravimetric analyzer (DSC-TGA Q600).

An argon flow rate of 100ml/min was used to prevent sample contamination from the measurement beams and to prevent the oxidation during and after DSC runs. The DSC tests were run at heating/cooling rates of 20°C/min over the temperature range of 50 to 580 °C. After heating, nitrogen-cooling was used for all runs for protection of specimen. Before each DSC run, the SDT Q600 TA Instrument was calibrated for TGA weight, DTA baseline, and temperature and DSC heat flow. Samples to be analyzed were put in an alumina cup on the sample beam, while an empty alumina cup was put on the reference beam. Right before or after each DSC run, a baseline run was required by running a separate test with two clean, empty alumina cups on the sample and reference beams. The DSC trace was then corrected by subtracting the baseline.

CHAPTER 4

RESULTS AND DISCUSSION

4.1 Characterization of hybrid preform

Figure 4-1 shows a hybrid preform made from the Al_2O_3 particles and fibres. The preform fabrication procedure is critical in determining the eventual properties of the magnesium composites. The SEM micrograph (Figure 4-2) depicts the microstructure of fibre preform; it clearly reflects the inter-fibre space in the pure fibre preform. The average inter-fibre spacing can be calculated using the equation as follow [66, 67]:

$$\lambda_f = (1-V_f)\, d_f\, /\, V_f \qquad\qquad \text{(Eq. 4-1)}$$

where d_f is the diameter of the fibers, V_f is the volume fraction of fibres.

If the V_f is 9%, and d_f is 5 µm, the λ_f can be worked out to be 50 µm. Figure 4-3 shows the microstructure of hybrid preforms including the particles and fibres. It can be seen from Figure 4-3 that the skeleton of fibres appear as a honeycomb structure that uniformly divided the preform into countless cells. The reinforced particles were dispersed and placed individually in the spacing of the cellular structure without agglomeration.

Examination of SEM micrographs showing the structure of the hybrid preforms manifests that, in the fabricating process, a three-dimensional skeleton as schematically illustrated in Figure 4-4 were constructed in which the fibres constituted a solid supporting frame, and the ceramic particles were homogeneously dispersed in this three-dimensional structure. The novel fabrication process of hybrid preform ensures that the reinforcements, both fibres and particles, disperse uniformly without agglomeration. Consequently, both the fibres and the particles can be dispersed in the matrix of composites in the subsequent process, which is the squeeze infiltration

of a magnesium alloy into the preform. At the same time, the space of each cell in the preform represents to a channel in which the molten magnesium alloy can flow, and which prevents the deformation of preforms and make the infiltration efficient. The contents, size and type of the ceramic reinforcement are selected with the definite quantity, and the shape of preforms. The developed process for the fabrication of hybrid preforms is flexible to combine different kinds of discontinuous ceramic reinforcements and matrices for a wide range of engineering applications. For example, the ceramic fibres would be alumina silicate fibre, alumina fibre, and monox fibre; the ceramic particles would be alumina particle, silicon carbide particle, alumina silicate particle, monox particle, and kubonit particle, and so on.

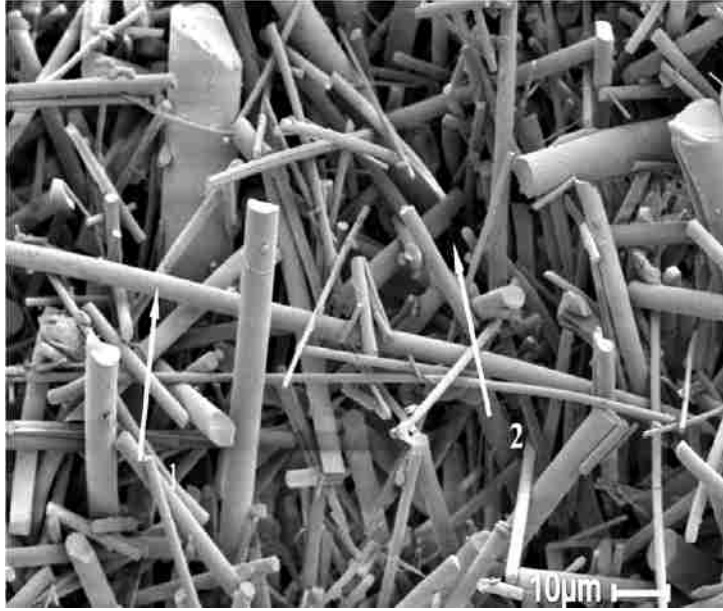Figure 4-1 A hybrid preform made from the Al_2O_3 particles (4vol %) and fibres (9vol %).

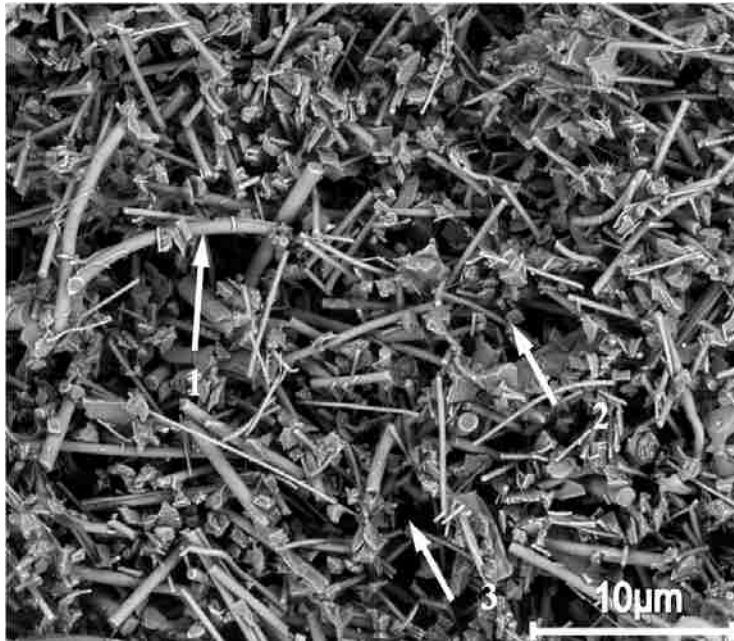Figure 4-2 SEM micrograph of pure fibre preform, Arrow 1- fibre and Arrow 2-empty cell.

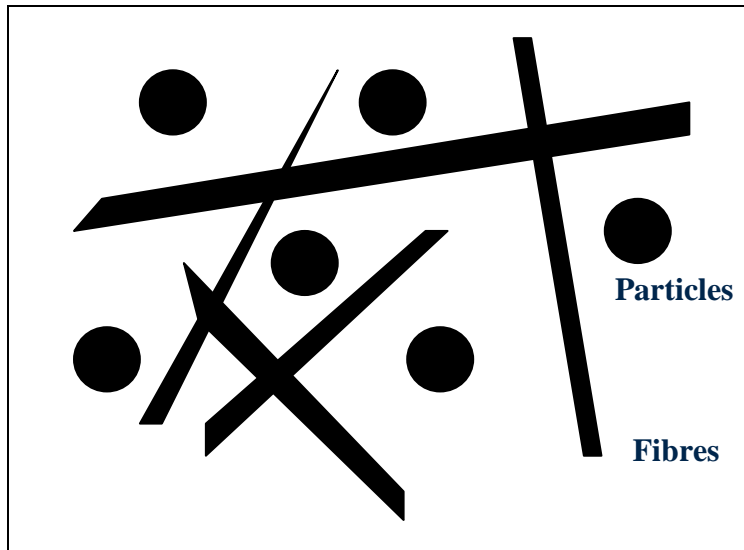Figure 4-3 SEM micrograph of hybrid preforms, Arrow1- fibre, Arrow 2-particle and Arrow 3-
empty cell.

Figure 4-4 Schematic illustration of the hybrid preform structure.

4.2 Characterization of Magnesium-based hybrid composites

4.2.1 Fabrication of hybrid composites

Figure 4-5 shows a sample of the squeeze cast hybrid composite. Molten matrix alloy infiltrates into a preheated preform under a certain pressure during the squeeze casting process. It has been reported [25] that the strength of the preform and the process parameters such as the preheated temperature of the preform, the pouring temperature of the matrix alloy, and the applied pressure level in the preform plus squeeze casting process, influence the quality and performance of the composites significantly. Here, the previous investigation (see section 3.4) will not be repeated, and optimized squeeze casting parameters for fabricating the composites will be discussed here in order to focus on understanding of the characteristics of the hybrid composites.

Figure 4-5 A squeeze cast hybrid composites (4vol. % Al_2O_3 particles + 9% vol. Al_2O_3 fibres)/

      AM60.

Y.Nishida [27] has described the threshold infiltration pressure, P_o, using the following equation during squeeze casting:

$$P_o = -[4V_f\gamma \cos\theta] / [d_f (1-V_f)] \qquad \text{(Eq. 4-2)}$$

where γ is the surface energy of the melt, θ is the contact angle between reinforcement and melt, V_f is the reinforcement volume fraction of the preform, and d_f is the diameter of the fibre or particle.

If it is under ideal conditions, when V_f =9%vol and d_f = 5µm, for the magnesium alloy which can improve the wetting and decrease the surface energy of the melt, the contact angle between reinforcement and magnesium alloy is less than 90°, the molten metal infiltrates the hybrid preform spontaneously. Generally, when modeling the infiltration, it is assumed that the preform does not deform. However, practically the liquid matrix is poured in under a certain

pressure to overcome capillary forces and other space resistance forces which, particularly with metallic matrices, oppose infiltration and can leave residual porosity. In fact, to obtain the high qualified and density composites, the final pressure can be as high as 90 MPa. These high pressures transmitted to the preform during the infiltration may cause it to deform, and result in undesired defects of the composites.

To optimize the applied pressure for preventing the deformation of hybrid preform, the compressive strengths of hybrid preform were evaluated by compressive tests at room temperature. Figure 4-6 shows a typical compressive engineering stress vs. strain curve for a hybrid preform (4%Particle + 9%Fibre).
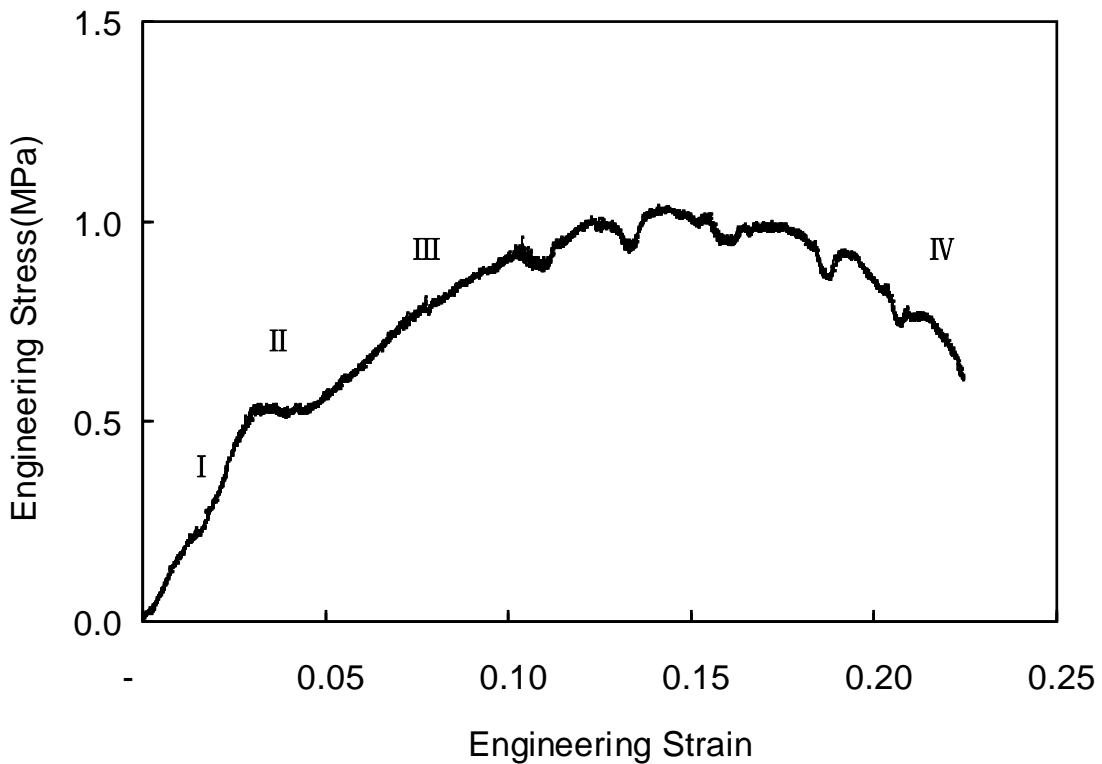
Figure 4-6 Typical compressive engineering stress vs. strain curve for a (4%Particle + 9%Fibre) hybrid preform.

In compression, there is a linear-elastic stage followed by a short plateau with a constant stress, and then the stress increases in a non-linear manners. This sequence of events repeats itself for cells until the specimen collapses. Each stage is associated with a specific mechanism of deformation.

The typical deformation sequence of the hybrid preform is revealed in Figure 4-7. Obviously, on first loading (I), the fibers bend giving linear elastic behaviour due to their linear elasticity of the fibres. The deformation was homogeneous throughout the specimen. (II)When a critical stress is reached, the deformation in the specimen begins to localize, which causes crack initiation by the brittle fracture mode. In compression the cells suffered progressive crushing, and cracks propagated catastrophically. (III) Eventually, at high strains, the cells collapsed sufficiently that opposing cell walls touch (or their broken fragments pack together) and further deformation compressed the cell walls. This gave the rising portion of the stress-strain curve labeled densification until specimen collapse.

The analysis of the stress-strain data reveals the critical stress P_0 of the developed hybrid preform is as low as 0.6 MPa. Beyond the critical stress, the deformation in the hybrid preform began to localize, the cellular structure of preform suffered progressive crushing, and the cracks propagated catastrophically. Because the fibres were brittle, it crushed and fractured in a brittle manner. Figure 4-8 shown the fracture of fibers is in a typical brittle manner, i.e., crush and cut.
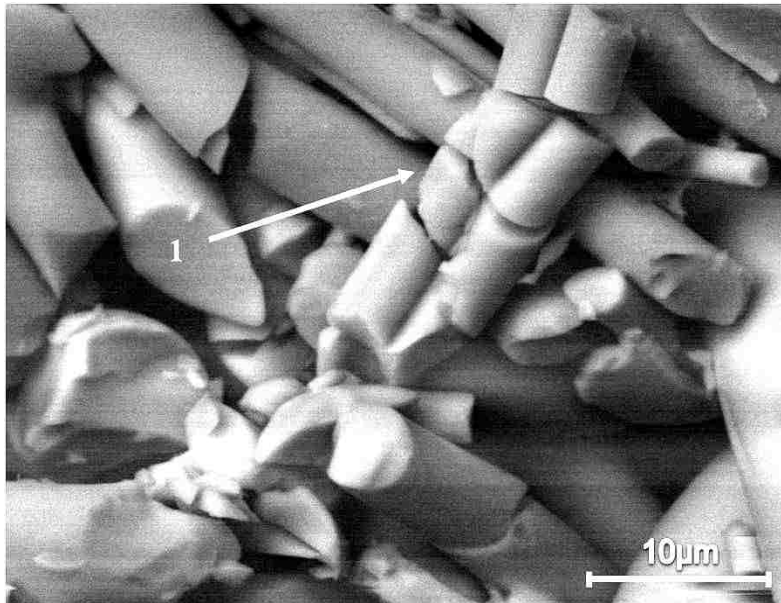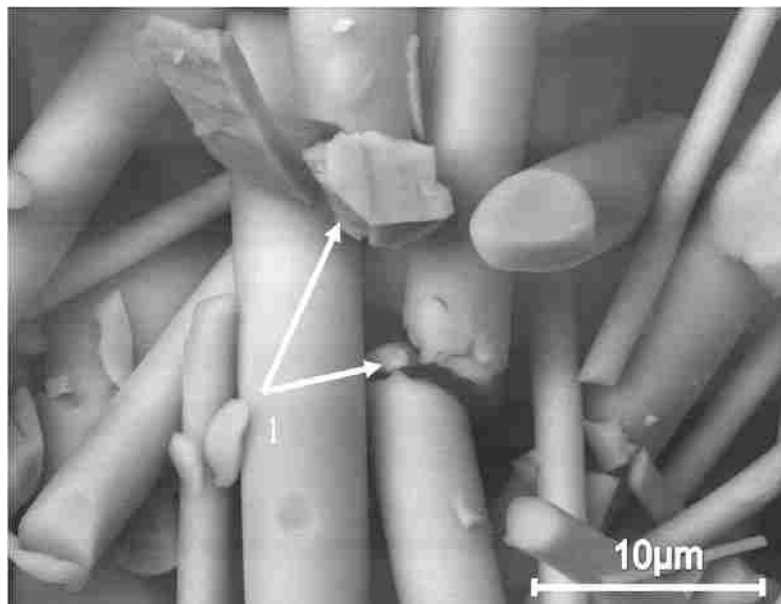
(I).

(II).
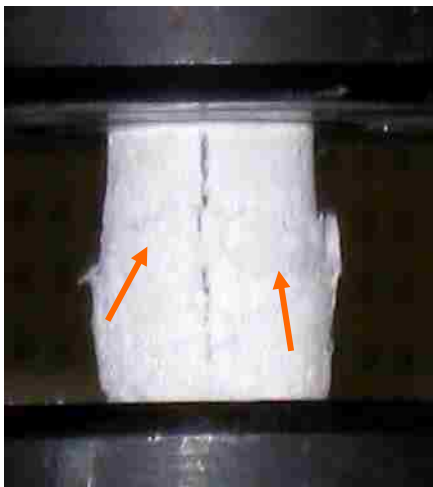
(III).

(IV).

Figure 4-7 Typical deformation sequence recording of the hybrid preform for the difference stages (Arrow: crack), Stage (I), stage (II), stage (III), and stage (IV).

(a)

(b)

Figure 4-8 Fractures of fibres preform, (a) Arrow 1-fibres crush and (b) Arrow 1-particles cut

down fibres.

To avoid the premature fracture of the preform, the pressure applied in the squeeze casting was increased gradually from a value below the critical stress. The gradual increase in the applied pressure as shown in Figure 4-9 effectively prevents the deformation of the preform during squeeze casting. The applied pressure during casting and infiltration enabled molten matrix alloy with relatively high superheat in the preheated die to flow into the preform and wet the reinforcement although no wetting agents were employed. Also, because the contact time between the molten alloy and the reinforcement at a high casting temperature was very short with the help of the applied pressure, the microstructure of the composites is homogeneous without the porosity and reactants.
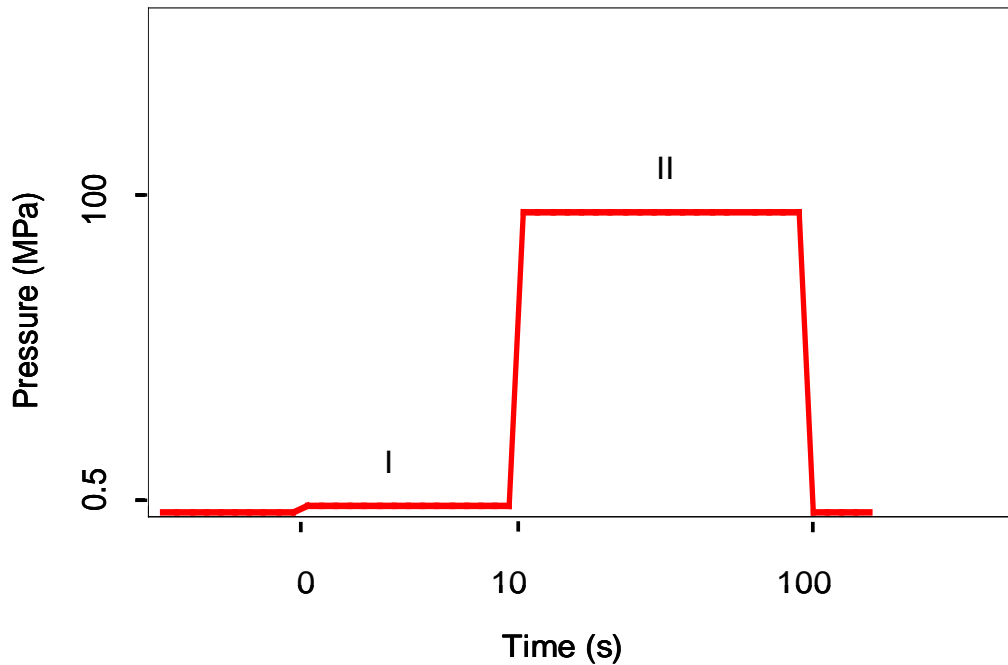

Figure 4-9 Two-step squeeze casting process, Step I- 0.5 MPa x10 s and Step II- 90 MPa x110 s.

4.2.2 Microstructural analysis

The microstructure analysis of the unreinforced AM60 in Figure 4-10 (a) indicates the presence of eutectic along the grain boundaries, within which is present the β-$Mg_{17}Al_{12}$. The precipitates are hard and brittle and have certain contribution to the hardness values. Figure 4-10 (b) illustrates that the short fibres are distributed in a random and isotropic orientation in the fibre-reinforced composites. The microstructure of the hybrid magnesium composite is given in Figure 4-10 (c). It can be seen that the fibres and particles are uniformly distributed throughout the matrix alloys. The addition of particles has almost no influence on the uniformity of fibres even if the particle content increases to 4 vol%. Voids can hardly be detected within the microstructure, indicating a high densification of the hybrid composites due to a gradual application of the infiltration pressure. It is also found that the matrix alloy has successfully infiltrated into the hybrid preforms. A heterogeneous distribution of reinforcements may degrade the mechanical properties of the composites and lead to an inhomogeneous grain size and defects of the composites. However, despite the large difference in size between the particles and the fibres, it is evident from Figure 4-10 (c) that the particles and fibres are dispersed uniformly without agglomeration and cave in the matrix alloy. The observed microstructure with both the ceramic particles and fibres distributed uniformly in the matrix alloy maximizes the benefits of the ceramic particles as the main reinforcement to enhance the mechanical and wear properties of the composites, and the fibres help to improve their toughness. The overall properties of composites are improved and can be optimized.
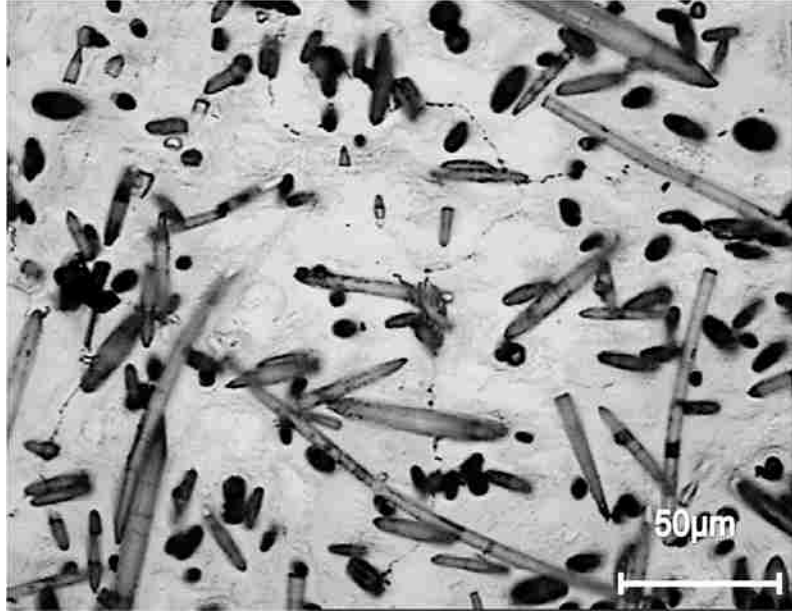
(a)

(b)

57
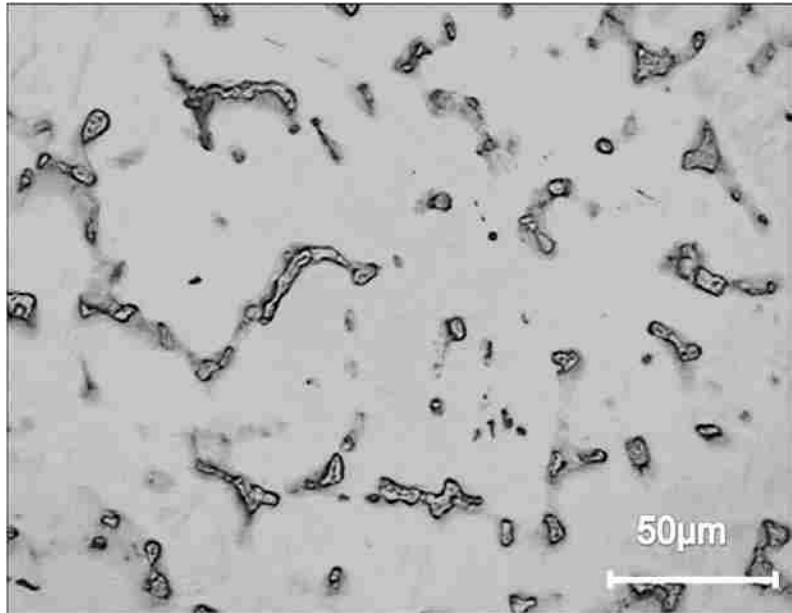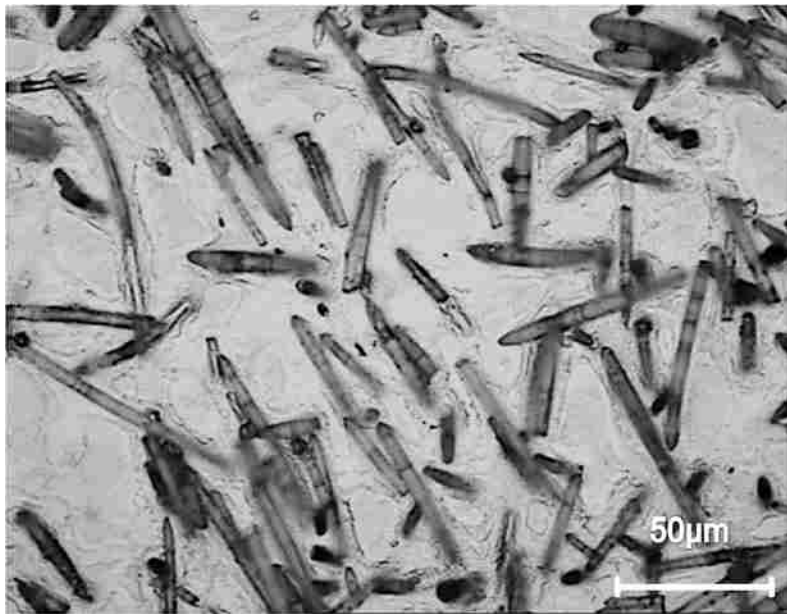
(c)

Figure 4-10 Optical photograph showing the microstructures of matrix alloy and composites, (a) AM60, (b) 9%Fibres/ AM60, and (c) (4%particles + 9%Fibres) /AM60.

4.3 Solidification of magnesium-based hybrid composites

4.3.1 Solidification behaviours of matrix alloy and its composites

Figure 4-11 represents the typical result of melting curves for AM60, F/AM60 and (P+ F)/ AM60. Two typical peaks are present on the cooling curves, i.e., peak 1 around 600°C, and peak 2 at 430°C. Based on the above curves, the solidification temperatures can be calculated and listed in Table 4-1.
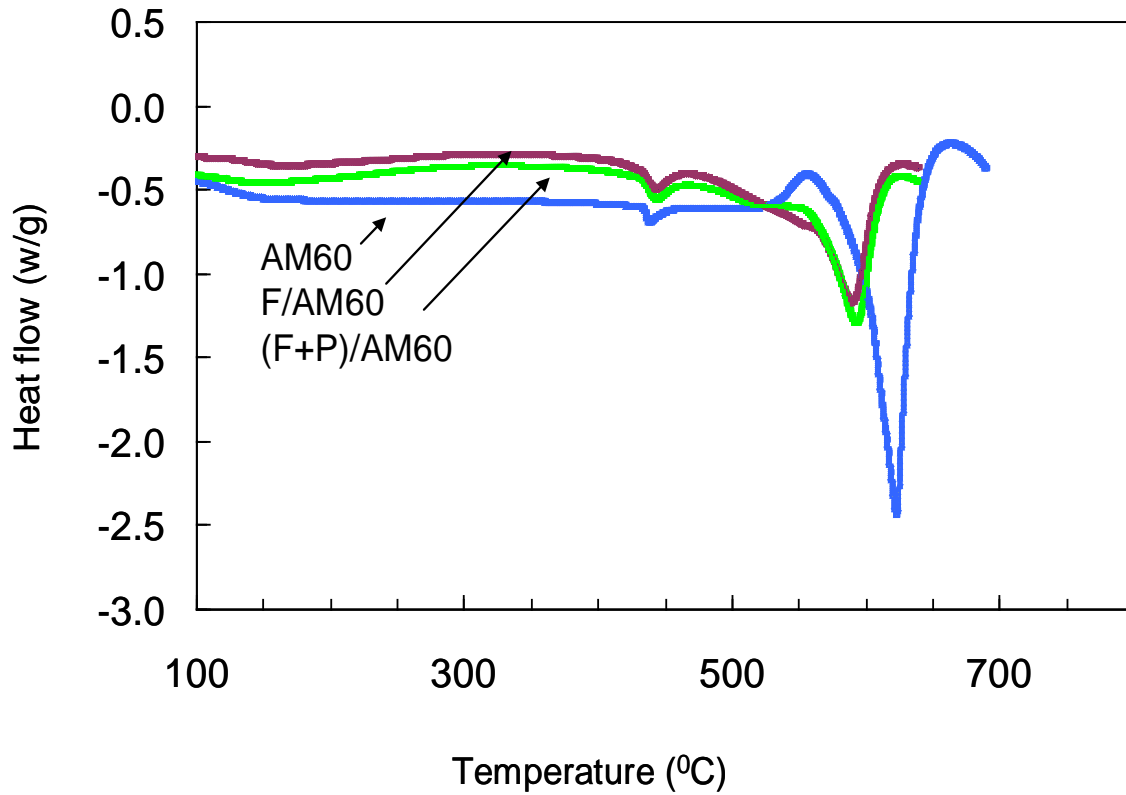
Figure 4-11 Typical result of melting curves for AM60, F/AM60 and (P+ F)/ AM60.

Table 4-1 Solidification temperatures of AM60, F/AM and (P+F)/AM60 in melting curves

Materials type	Peak 1--- primary Mg (^{o}C)			Peak 2--- eutectic phase (^{o}C)		
	Initial (T_o)	Peak (T_p)	End (T_e)	Initial (T_o)	Peak (T_p)	End (T_e)
AM60 alloy	554.80	623.64	659.31	431.22	437.86	454.78
F /AM60	556.70	587.98	620.32	433.71	441.17	460.25
(P+F) /AM60	555.63	593.78	622.81	435.37	442.00	462.74

Obviously, at peak 1, the onset solidification temperature of the matrix AM60 melting is higher than that of the fibre-reinforced AM60 composite. In addition, the onset solidification temperature of the (F+P)/AM60 composite is between those of the F/AM60 and AM60. This observation implies that particles possibly play a different role in the solidification behaviour of the composites compared with the fibres.

Peak 2 corresponds to incipient melting zones where Al content exceeds solid solubility limits (about 12 mass %) having eutectic structure. This fact, supported by T_p, is very close to $437^{o}C$ which is the melting temperature of the eutectic phase $Mg_{17}Al_{12}$. It is observed that the onset eutectic melting temperatures of (F+P)/AM60, F/AM60 and AM60 are $435.37^{o}C$, $433.71^{o}C$, and $431.22^{o}C$, respectively. The data clearly show that the nucleation of the eutectic phases was accelerated in the composites since the addition of the fibers and particles led to an increase in the onset eutectic melting temperature. As a result, it was reasonable to deduce that both fibres and particles play an important role in the nucleation and growth of the eutectic phase.

In order to further investigate the solidification processes of magnesium (AM60) alloy and its composites, the cooling curves of the materials were measured. Figure 4-12 represents a typical result of the thermal analysis for AM60, F/AM60 and (P +F)/AM60.

Examination of the cooling curve shown in Figure 4-12 indicates two distinct stages during the solidification process of the AM60 alloy and its composites. Figure 4-13 was an enlargement of the parts of the two different stages. The two stages of cooling curves are matched to two peaks on the melting curves.
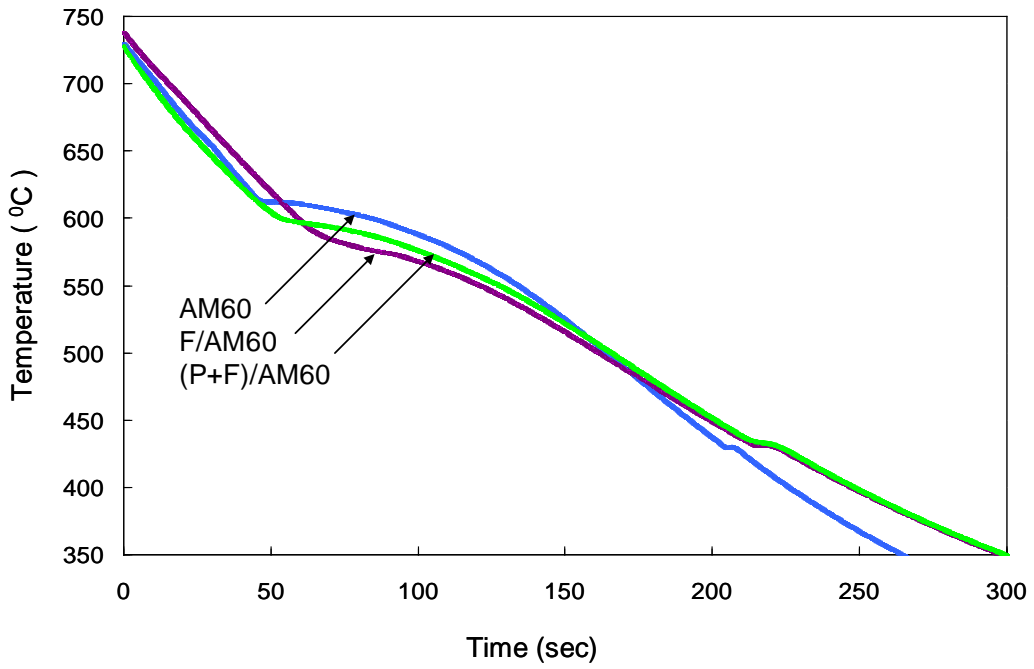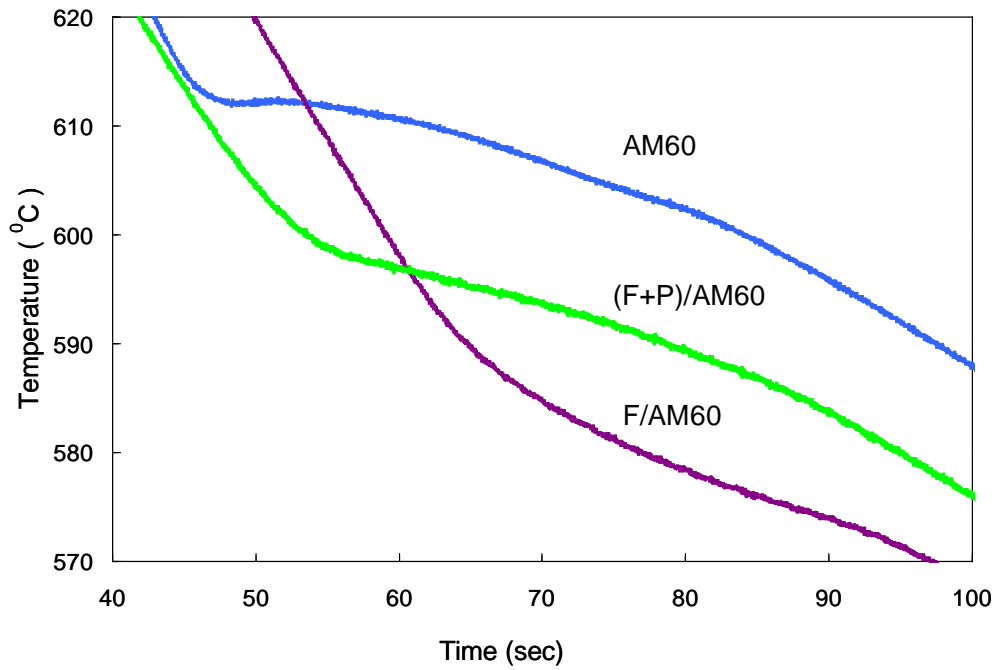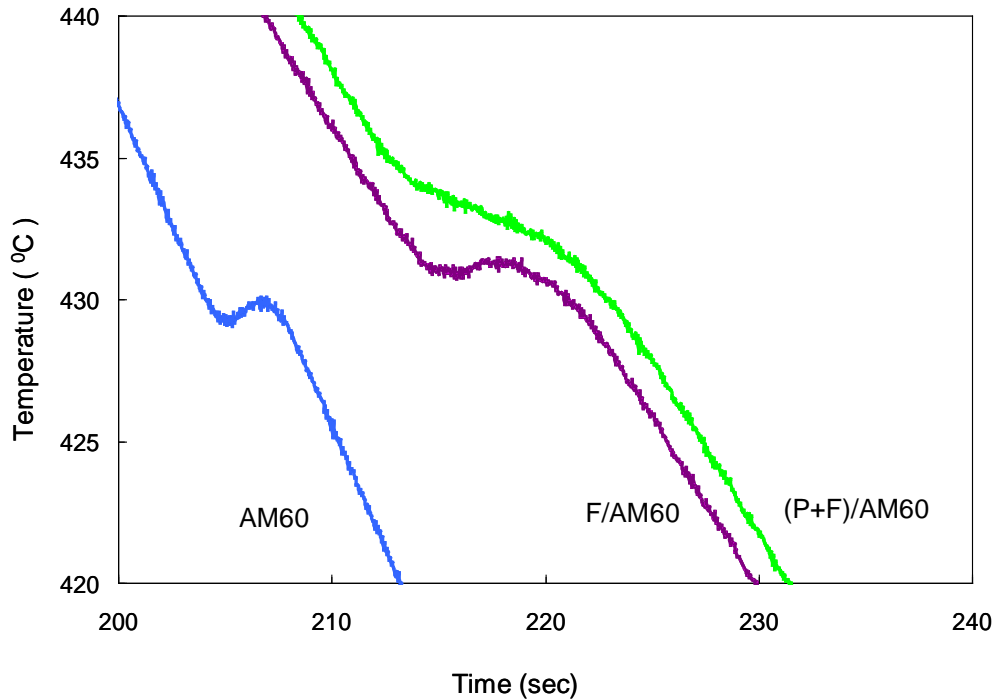
Figure 4-12 Typical cooling curves of AM60 and its composites.

(a)

(b)

Figure 4-13 Enlarged parts of the cooling curves, (a) Stage 1, primary α–Mg nucleation, and (b) Stage 2, nucleation of the eutectic phase.

In the case of the AM60 alloy, the nucleation of the primary magnesium phase happened in Stage (1) with the non-equilibrium liquid temperature of 612-612.5°C. Stage (2) is the occurrence of the eutectic reaction, i.e. L →α-Mg + Mg$_{17}$Al$_{12}$, where the non-equilibrium solids temperature was determined as 429.2-430°C. The enlarged cooling curve shown in Figure 4-13 evidently gives the degree of supercooling (ΔT=0.5°C) at the liquid temperature plateau, and at Stage (2) ΔT=0.8°C.

For the F/AM60 and (P+ F)/AM60 composites, however, no apparent supercooling is observed at Stage (1). F/AM60 composite exhibits a slight supercooling (ΔT=0.4°C) at Stage (2) compared with the AM60 alloy. No supercooling is seen for (P+ F) /AM60 composites. The

difference in supercooling appearance between the AM60 alloy, Fiber/AM60, and (P+ F)/AM60 composite can be directly attributed to the mechanism of the primary phase nucleation, eutectic phase nucleation, and consequently, the extent of grain refinement.
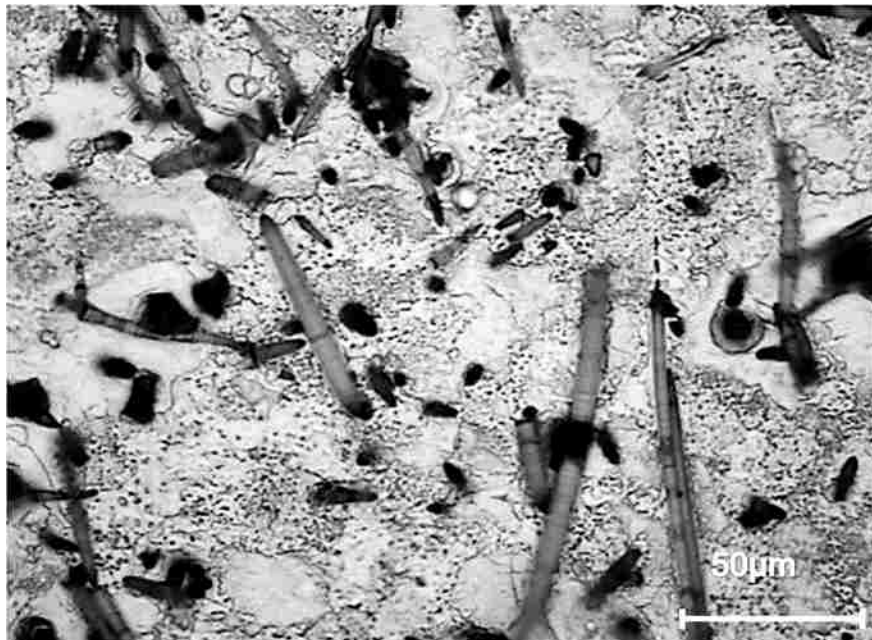
Figure 4-14 gives the grain structures of the matrix alloy and the composites. The grain size measurements for the composites and unreinforced AM60 matrix alloy are presented in Figure 4-15.
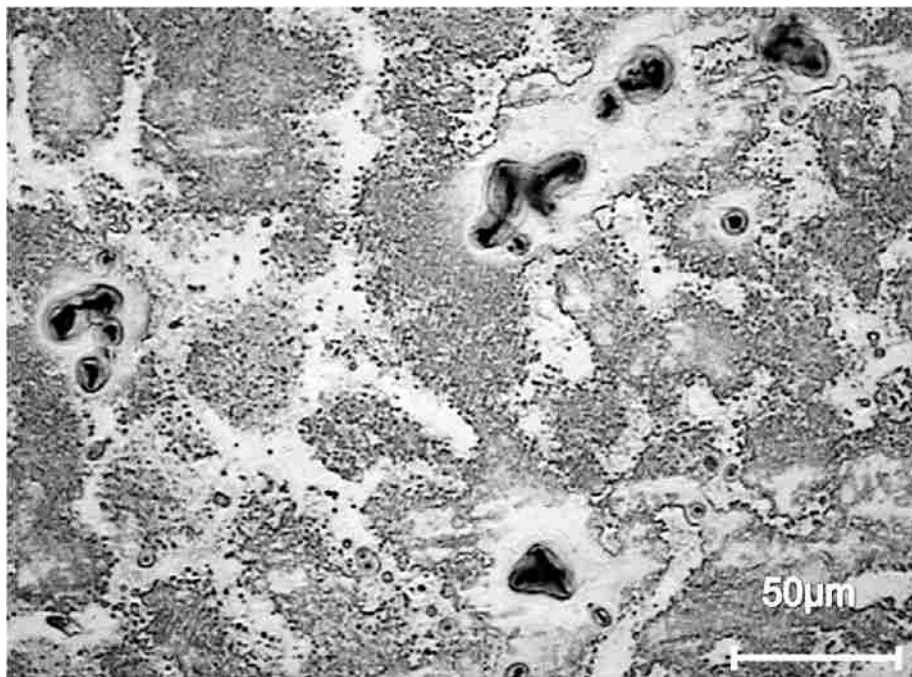
(a)
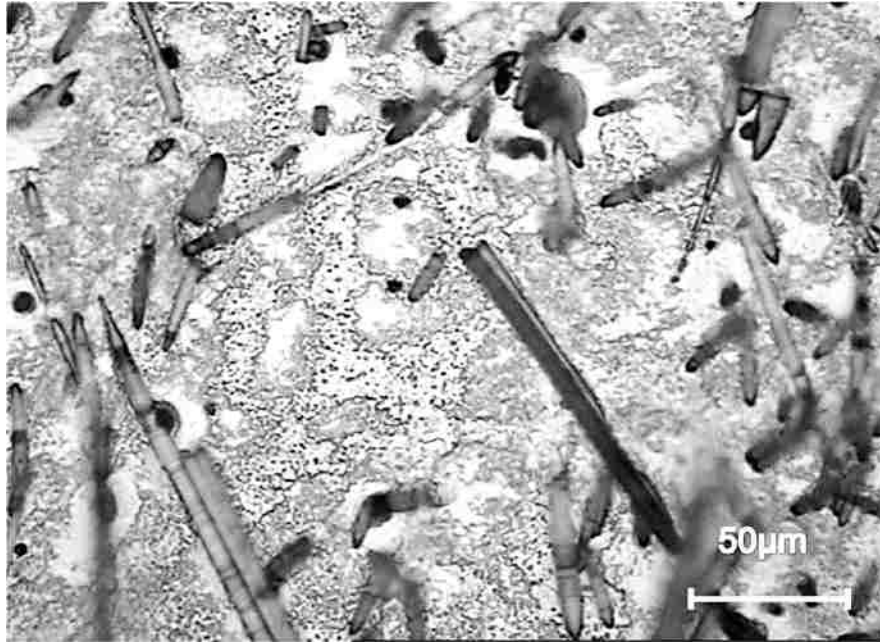
(b)

(c)

Figure 4-14 Optical micrographs showing grain structure of (a) unreinforced AM60 matrix alloy,

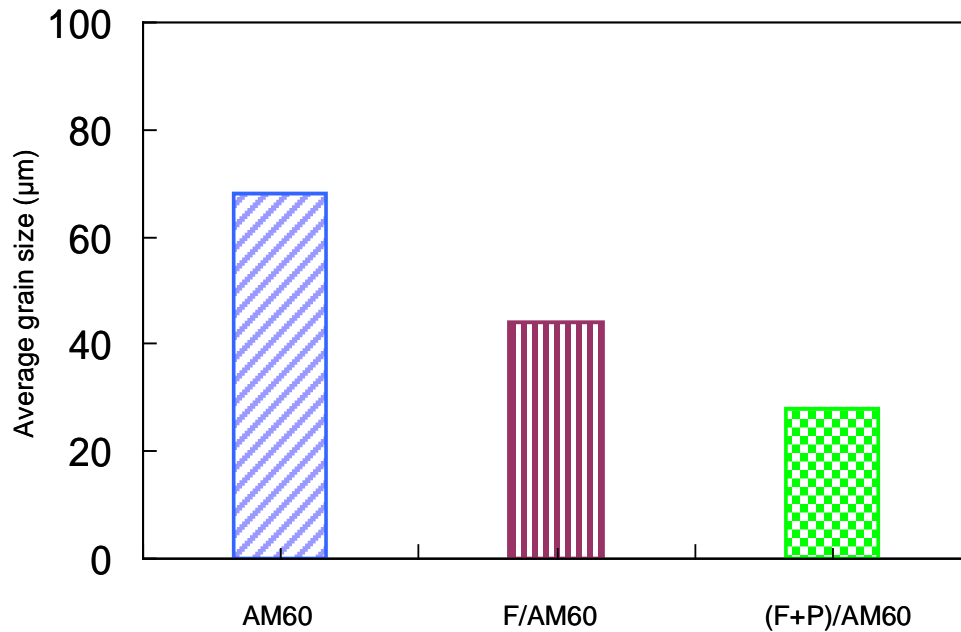(b) F/ AM60, and (c) (P+F)/ AM60 (All are under T4 condition).

Figure 4-15 Measured grain size of the matrix alloy, F/AM60 and (F+P)/AM60 composites.

From Figure 4-14, an evident difference in grain sizes between unreinforced AM60, F/AM60 and (P + F)/AM60 can be seen. This implies that the addition of fibres and particles leads to a finer grain structure in the composite. As can be seen, the grains in the matrix of the F/AM60 and (P+ F)/AM60 are refined. Figure 4-15 presents the grain size measurements for both the unreinforced AM60 alloy and its composites. It is worth noting that the grain size of the AM60 alloy matrix is reduced by more than three times in the hybrid composites due to the grain refinement effect of the hybrid reinforcements.

4.3.2 Grain refinement mechanisms

Obviously, the supercooling of magnesium alloys can be correlated to their grain structure. Metals that would give coarse grains yield high supercooling, and melts with low or no super-cooling give rise to fine grains. The reason is that the grain nucleation in a solidification liquid alloy is difficult to initiate when heterogeneous nuclei are absent. As such, the melt needs to supercool until appropriate nuclei form. At the beginning of the nucleation, the melt temperature increases and the grain growth occurs at the normal equilibrium temperature. With the reinforcement addition, the number of nuclei and the nucleation rate increases. As a result, small or no supercooling appears on the cooling curve as the fine grained structure is achieved. The results of thermal analysis acquired in this study conform to the principles of the nucleation theory [58].

The unreinforced AM60 alloy which has coarse grains gives $0.5^{o}C$ of supercooling on its cooling curve. Meanwhile, no supercooling is exhibited by the particle and fibre reinforced AM60 composites in which the grain refinement takes place.

It is known that both Al_2O_3 particles and fibres have a lower thermal conductivity and heat expansion coefficient than the magnesium melt. Thus, the magnesium melt that surrounds the Al_2O_3 fibres has a lower cooling rate compared with the matrix alloy, and the solidification of the magnesium melt surrounding the Al_2O_3 fibres is retarded. It appears that Al_2O_3 short fibres may not serve as a heterogeneous nucleation site for primary Mg since the fibre-reinforced composite exhibits a liquidus temperature higher than that of the matrix. Nucleation of primary Mg most likely takes place in the space between the fibers. The measured grain size of the fibre-reinforced composite evidently matches the calculated average inter-fibre spacing, which is

around 50 μm. Obviously, it is not the short fibres themselves but the spaces in the fibre-preform structure that restrict grain growth.

The onset solidification temperature of the (F+P)/AM60 composites is at the middle of F/AM60 and AM60, revealing that particles play a different function in the composites compared with fibres. It has been reported [37] that the addition of reinforcement results in a reduction in grain size in AM50 alloy. The observed grain refinement are primarily due to the combined effect of heterogeneous nucleation of primary magnesium on Al_2O_3 particles, and restricted growth of magnesium grains, and heterogeneous nucleation of eutectic magnesium ($Mg_{12}Al_{17}$) on Al_2O_3 particles and fibres. This is also supported by a previous study [63] that primary phase nucleates preferentially on the surface of particles. The optical micrograph in Figure 4-16 shows that the coupled effect of the heterogeneous nucleation of the primary magnesium phase on Al_2O_3 particulates, and the restricted growth of magnesium crystals, may be responsible for the formation of small grains in the hybrid composite. Moreover, since Al_2O_3 particles are generally polycrystalline, the exposed atomic planes may not always be able to serve as substrates for the heterogeneous nucleation of the primary magnesium phase. This helps to explain why particles were pushed by the primary phase into the last freezing zone in the magnesium composites.

However, the situation is changed at the eutectic phase ($Mg_{17}Al_{12}$). An increase in the eutectic melting temperatures of (F+P)/AM60 and F/AM60 indicates that both fibres and particles could become heterogeneous nucleation sites for the eutectic phase. This is further evidenced by the optical microstructure analysis in Figure 4-17 showing nucleation sites provided by the fibres and particles to facilitate the solidification of the eutectic phase. In Figure 4-17, it is observed that eutectic phase attaches to the surface of the reinforcement, and nucleates and grows on the reinforcement. The evidence of heterogeneous nucleation of the eutectic phase

on reinforcement may be attributed to the relationship of coherent interface between the eutectic phase and the reinforcement. Obviously, eutectic phases are able to wet both Al_2O_3 fibres and particles. As a result, they can heterogeneously nucleate on both the Al_2O_3 particles and fibres substrate. The defects in the Al_2O_3 particles and fibres - such as stacking faults, dislocations, and pits or grooves - would also act as favorable sites for heterogeneous nucleation.

An interesting phenomenon is observed on the cooling curves in that both AM60 and F/AM60 composites show a difference in the degree of supercooling at stage (2) of Figure 4-13, which is related with the eutectic phase formation in the magnesium alloy. Although fibres serve as heterogeneous nucleation sites for the eutectic phase, it does not have a significant influence on the refinement of the eutectic phase, and this is assisted with the observation of microstructure observation of composites.

The mechanism for grain refinement of the matrix of metal matrix composites has been investigated. Primarily, grain refinement results from two separate processes: nucleation of new crystals from the melt, and subsequent growth of the new crystals to a limited size. Although heterogeneous nucleation enhances the rapid creation of primary crystals, the onset of the primary phase nucleation should not be followed by rapid crystal growth.

Besides the structure of the fibre preform limiting the growth of the primary magnesium, the presence of particulates inside the primary magnesium grains and at the grain boundaries suggests that both particle capture and pushing occurred during the solidification of the composites.
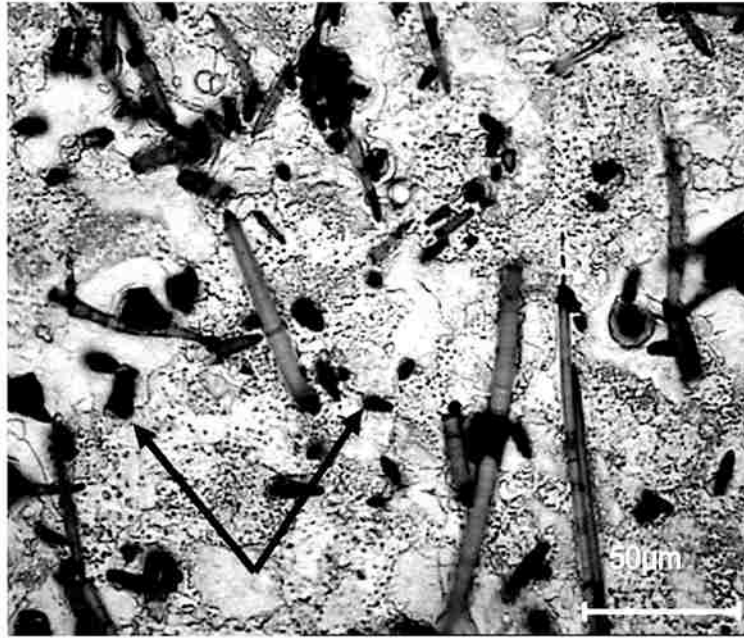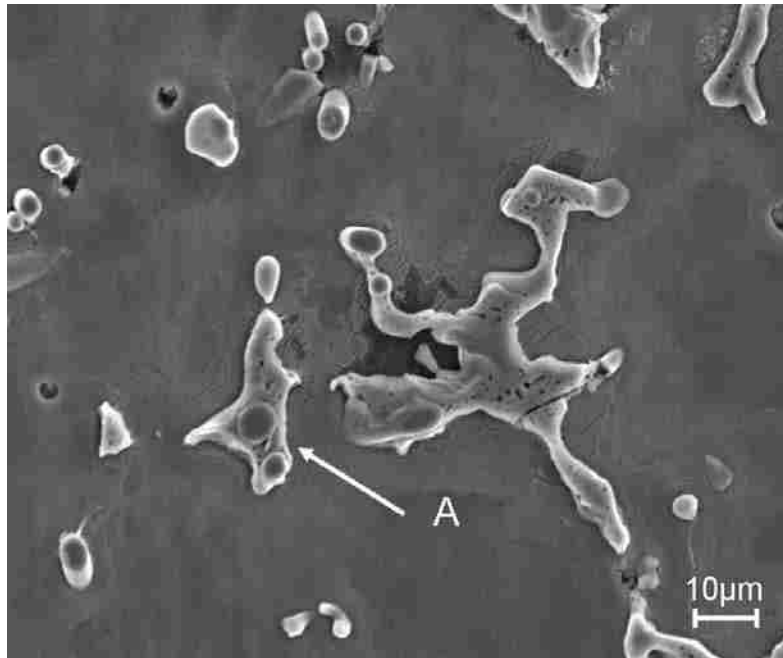
(a)
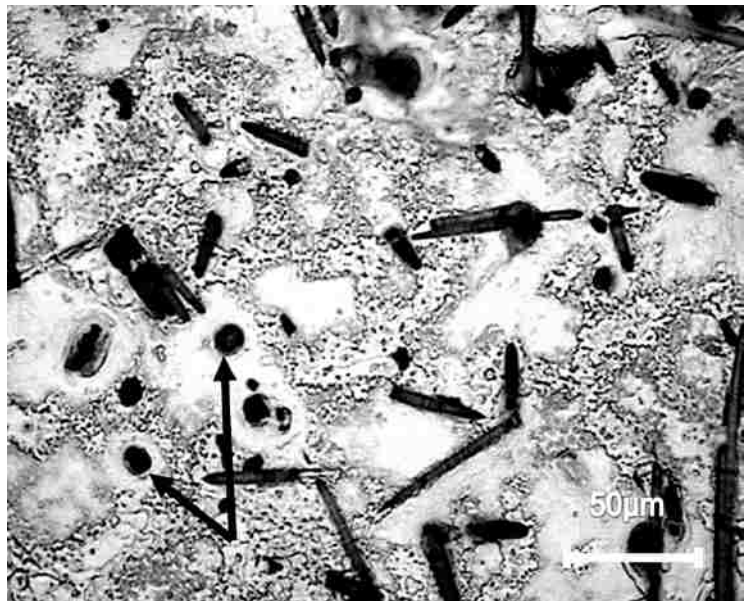
(b)

Figure 4-16 Coupled effects of the heterogeneous nucleation of the primary magnesium phase, (a) Arrow -the Al_2O_3 particulates restrict growth of magnesium crystals and (b) Arrow - the heterogeneous nucleation of the primary magnesium phase on Al_2O_3 particulates.

(a)
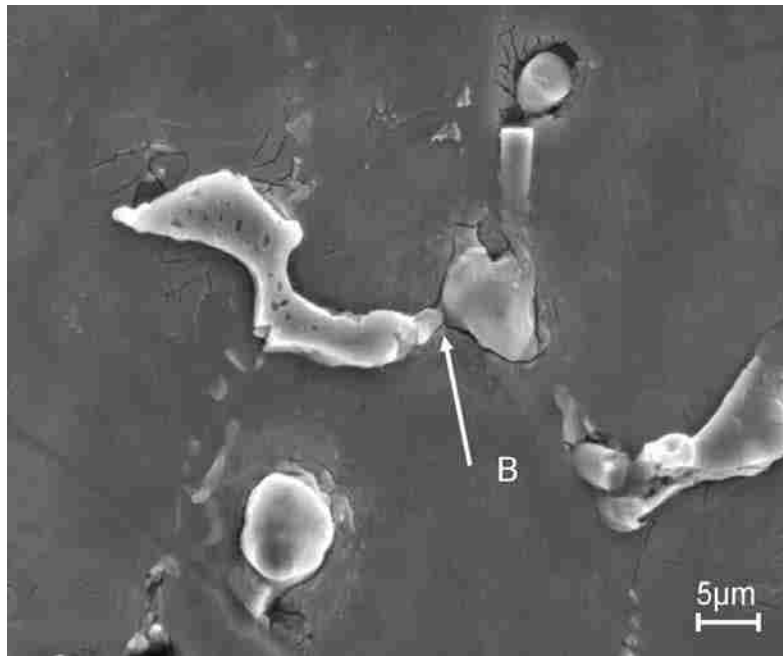
(b)

Figure 4-17 Fibre & particle serve as nucleation of eutectic phase, (a) Arrow A-fibre is heterogeneous nucleation substrate and (b) Arrow B-particle is heterogeneous nucleation substrate.

This interpretation is evidently supported by the optical observation on the heat-treated composite specimen as indicated in Figure 4-16. It appears that particulates are situated inside the primary magnesium grains. This observation implies that heterogeneous nucleation may occur during the solidification of the composite. On the other hand, a significant particle pushing effect is suggested by the appearance of many particulates around the grains indicating that the growth rate of the primary phase may be reduced when the composite solidifies. This is because particulates present around the growing primary magnesium crystals could act as diffusion barriers to their growth. Consequently, the restricted growth of the primary phase would allow the melt to have sufficient time to create more nuclei. Therefore, it can be deduced from the experimental evidence that, for the hybrid composite, a fine grain size in the resulting solidified microstructure is attributable to both the heterogeneous nucleation and the restricted primary crystal growth. Also, it should be pointed out that the fibre-influenced heat accumulating capability of the preforms due to low thermal conductivities of reinforcements is one of the dominant factors controlling heat transfer during the solidification process. However, the particles play the main role for grain refinement during the solidification of the primary Mg in the hybrid composites

4.4 Mechanical properties of the composites

4.4.1 Hardness

The Rockwell harnesses of the matrix alloy and composites were measured to determine the influence of reinforcement on the magnesium and the isotropy of fibre and particle distribution. Hardness measurements were conducted using the Rockwell F scale for both the alloy and composites. The preference for the Rockwell rather than Vickers hardness scale was

due to the larger indentation needed to ensure a consistency in the measurements of the composites. The relatively small area of the Vickers indents, of which the measurement could be taken directly from the hard reinforcements, causes large variations in hardness values. The results of the macro-hardness measurements reveal an increase in material hardness with the presence of Al_2O_3 fibres and particles as shown in Figure 4-18.
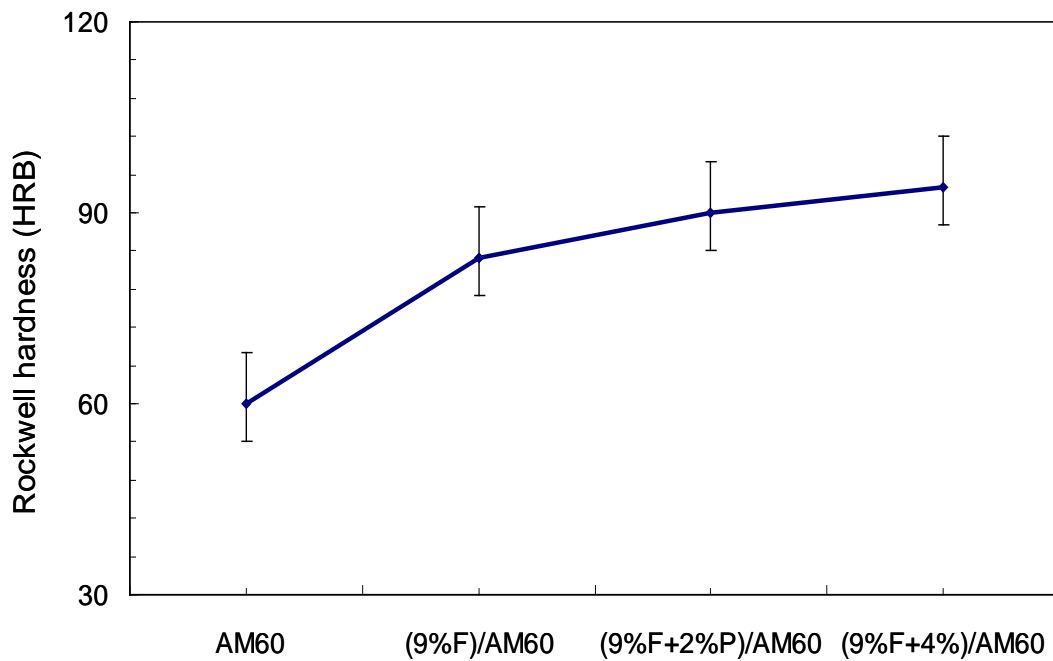

Figure 4-18 Hardness measurements for the matrix alloy and composites.

The increased hardness can be attributed primarily to the relatively harder ceramic particulates and fibres present in the matrix and to a higher constraint on the localized matrix deformation during indentation due to the presence of particles and fibres, and also due to the reduced grain size.
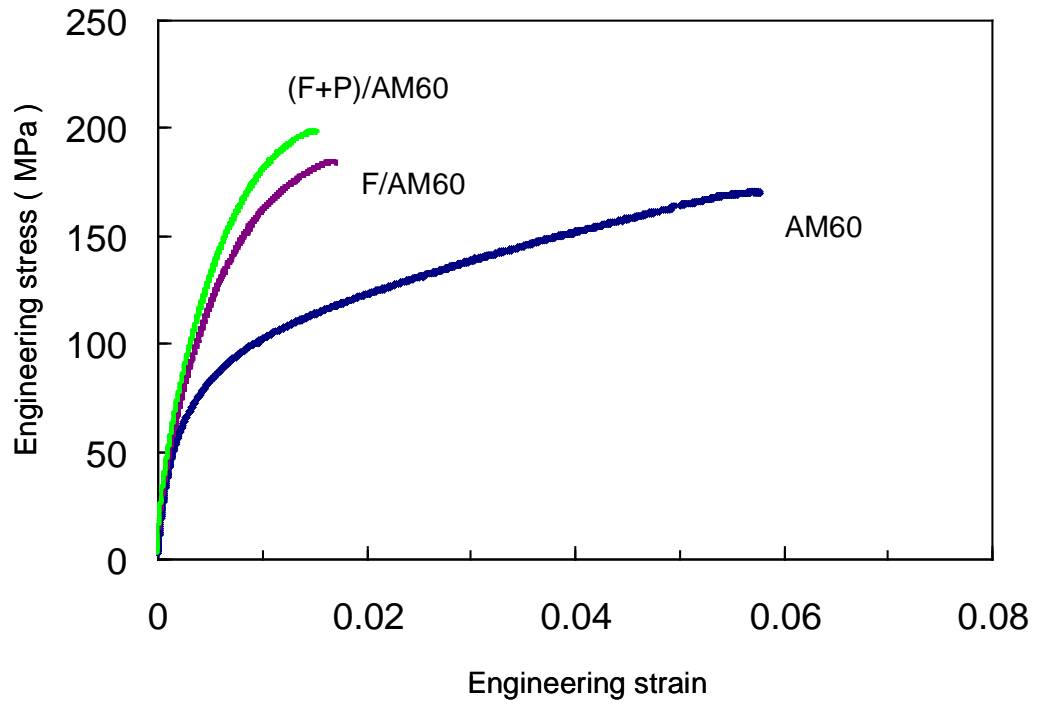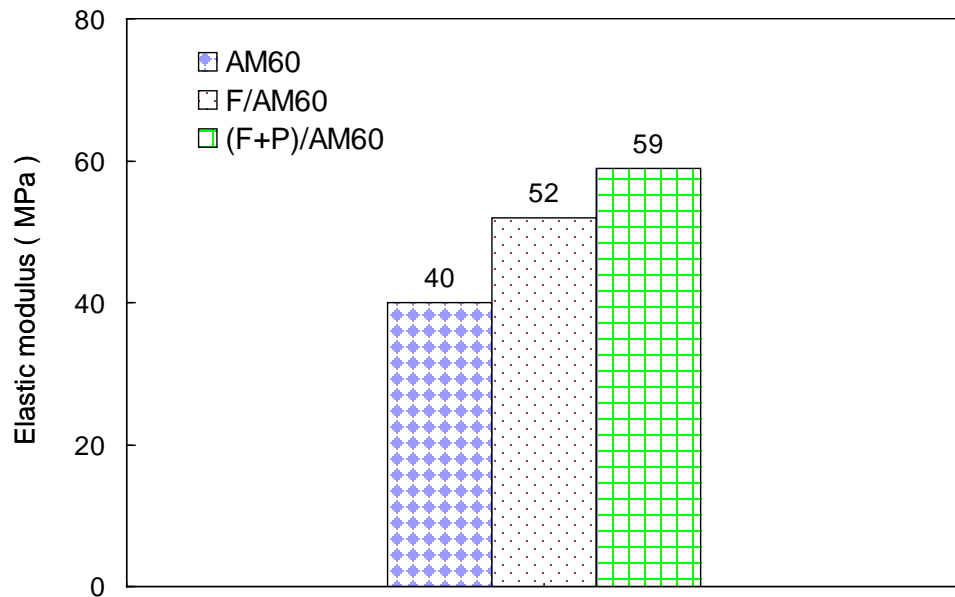
4.4.2 Tensile properties

Figure 4-19 Typical engineering stress vs. strain curves for AM60 ally, F/ AM60, and (P +F)/
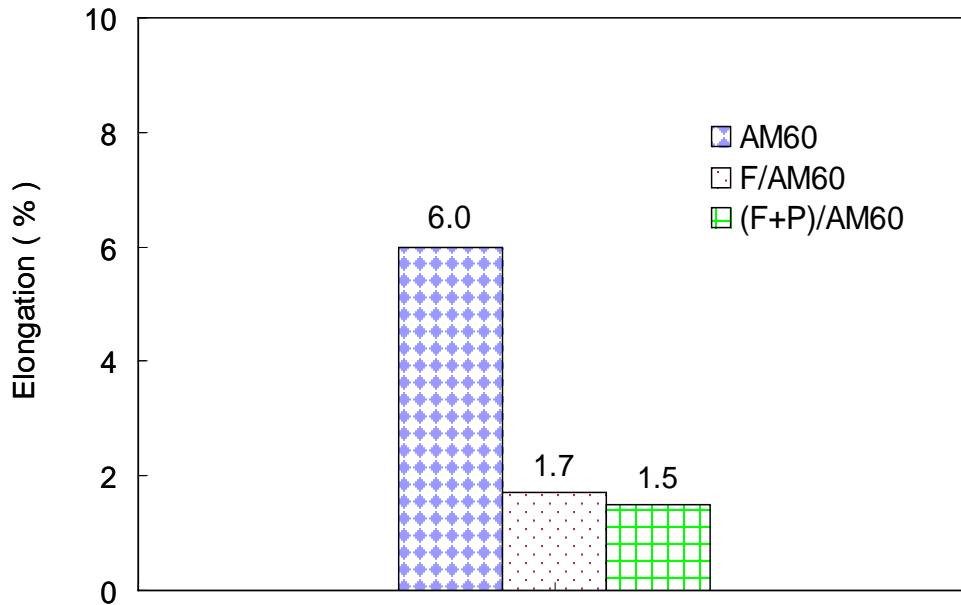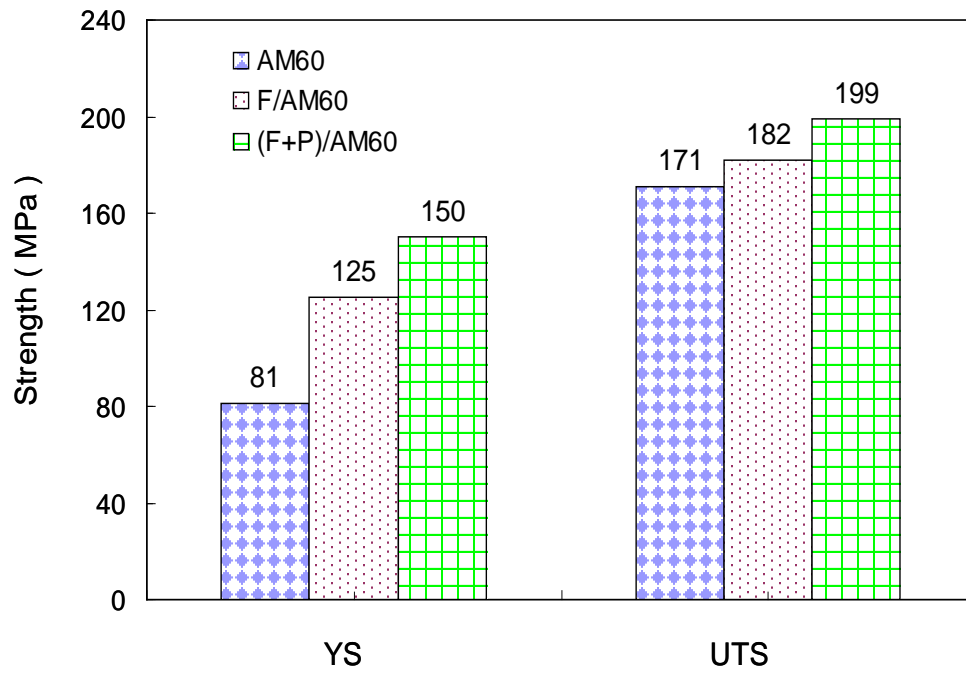
AM60 composites.

Figure 4-20 Tensile properties, Elastic modules, UTS, YS, and Elongation of AM60 alloy, F/

AM60, and (P +F)/ AM60.

The typical engineering stress-strain curves obtained from tensile testing of the squeeze cast AM60, F/ AM60, and (F+P)/ AM60 composites are shown in Figure 4-19 and the corresponding tensile mechanical properties are given in Figure 4-20. It can be seen from Figures 4-19 and 4-20 that the addition of reinforcements leads to a significant improvement in the elastic modulus and the strength, but results in a marked reduction in elongation. The yield strength (YS) of the composites, which are 125 and 150MPa for F/AM60 and (F+P)/AM60 respectively, are significantly improved, almost 88% over the unreinforced magnesium alloy. The elastic modulus (E) of the composites are 52 and 59GPa for F/AM60 and (F+P)/AM60, respectively, which is 30% and 40% higher than that (40GPa) of the matrix alloy. The ultimate tensile strength (UTS) of the two composites is 182MPa for F/AM60 and 199MPa for (F+P)/AM60 respectively, which leads to an increase of 6% and 16% higher than that of the matrix alloy AM60 (172MPa). Compared to that (6%) of the matrix AM60 alloy, the elongation to failure (e_f) of the composites are 1.7% and 1.5% for the F/AM60 and (F+P)/AM60 composites respectively. No necking phenomena were observed for the composites prior to fracture due to their low ductility, while a slight but notable necking was observed for the squeeze cast AM60.

The true stress-strain can be determined from the engineering stress-stain by the follows:

$$\sigma_t = \sigma_e \ (\ 1 + \varepsilon_e \ ) \tag{Eq.4-3}$$

$$\varepsilon_t = \ln \ (\ 1 + \varepsilon_e \ ) \tag{Eq.4-4}$$

where σ_t is the true stress, ε_t is the true stain, σ_e is the engineering stress, and ε_e is the engineering strain.
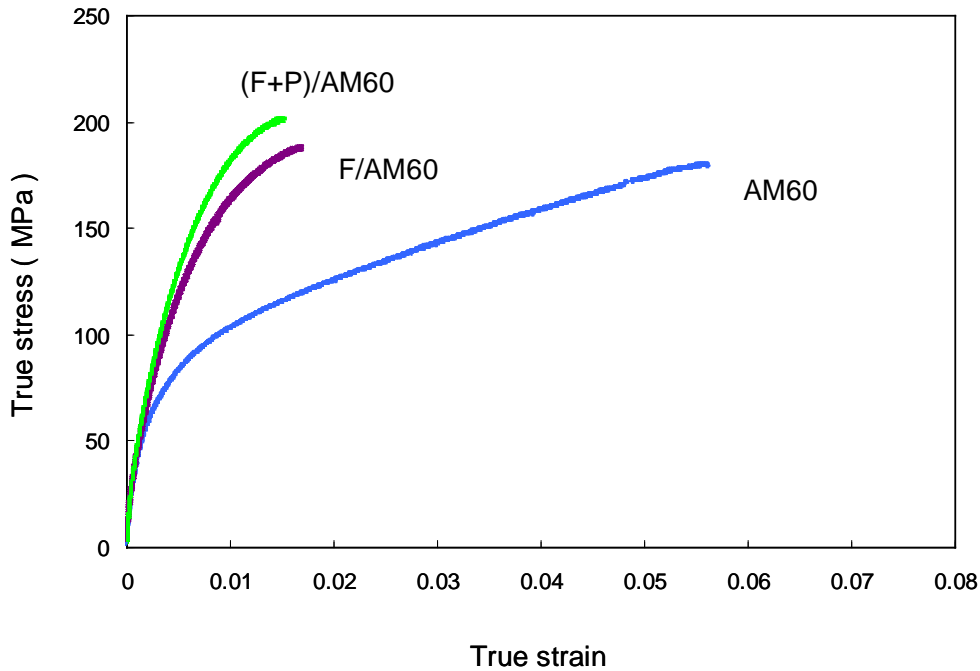
Figure 4-21 Typical true stress vs. strain curves for AM60 ally, F/ AM60, and (P +F)/ AM60 composites.

Figure 4-21 shows representative true stress and strain curves of AM60 alloy, F/ AM60, and (P +F)/ AM60 composites. For all three materials, the stress varies with the strain in a similar pattern. Under tensile loading, the materials deformed elastically first. Once the yield point is reached, plastic deformation follows. However, the (P +F)/ AM60 composites fractured at high-stress and low–strain levels compared to the F/ AM60 and AM60 alloy.

The stress-strain curve for metals is often described by the power law [68]:

$$\sigma = K \varepsilon^{n}$$
(Eq. 4-5)

where K and n are empirical constants.

The regression analysis indicates that the power law is in good agreement with the tensile results. The numerical values of these constants in above equation with the regression

coefficients are listed in Table 4-2. The above equation can be differentiated to obtain strain-hardening rates (dб/dε).

Table 4-2 Best fit parameters for power equations

Material types	K (MPa)	n	R^2
(P +F)/ AM60	1627.8	0.483	0.972
F/ AM60	1303.4	0.458	0.979
AM60	393.5	0.295	0.991

The strain-hardening behaviour of the alloy and composite can be clearly shown in a plot of stain-hardening rate (dб/dε) vs. true plastic strain during the plastic deformation as shown in Figure 4-22, which is derived from Figure 4-21. The (P +F)/ AM60 composite has a high strain-hardening rate (19000 MPa) with respect to the AM60 specimen (9300) at the onset of plastic deformation. It is evident that, for all three materials, their strain-hardening rates decrease with increasing true strain. Moreover, the strain-hardening rate during the plastic deformation of the materials varies also with reinforced particles and fibres. As the particles add into materials, the strain- hardening rate increases significant. This observation implies that, compared to the AM60 samples, the F/AM60 and (P+F)/ AM60 composites are capable of spontaneously strengthening itself increasingly to a large extent, in response to lose a slight plastic deformation prior to fracture. Obviously, it is reinforced particles and fibres that are main influencing factors in increasing strain-hardening rate of composites, compared with AM60 matrix alloy, during the plastic deformation. The reinforced particles and fibres inside grains and ground grain boundaries observed in the following fracture behaviour analysis, which resist slip in the primary

phase, should be responsible for the relatively strain-hardening rate of the composites in the early stage of plastic deformation, that is, instantly after the onset plastic flow in Figure 4-22.
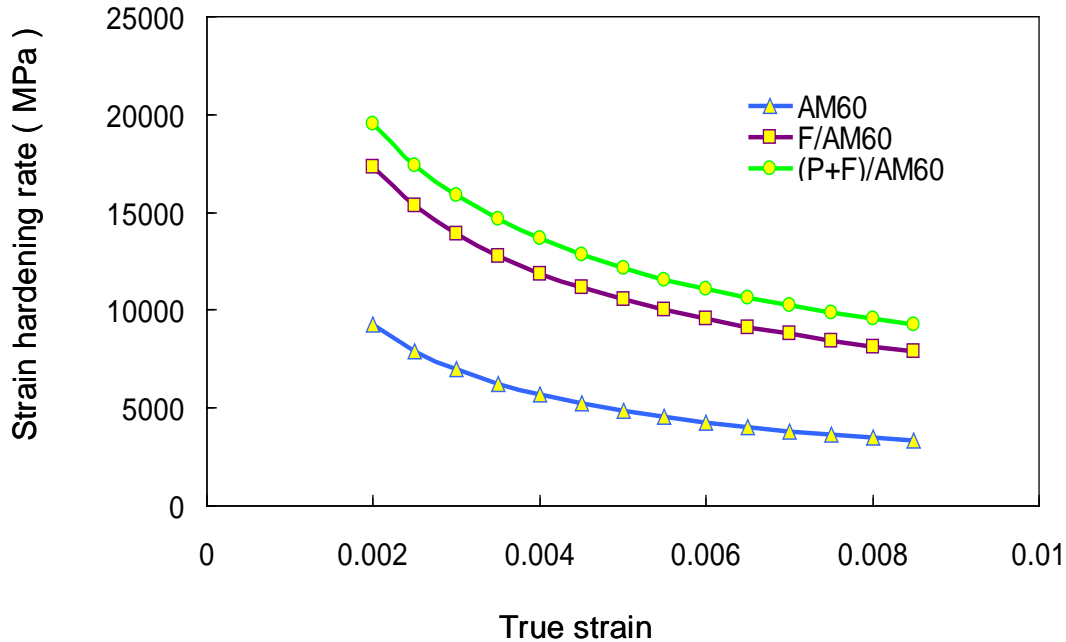

Figure 4-22 Strain-hardening rate vs. true plastic strain curves for unreinforced AM60 matrix alloy and its composites.

4.4.3 Fracture Behaviour

The differences in the fracture behaviours between the matrix alloy and hybrid composites are evidently revealed in Figures 4-23 and 4-24 by the SEM fractography. Figure 4-23 shows the typical fracture surface of the AM60, which is primarily ductile in nature. The observed fracture mode of the squeeze cast specimens in as-cast conditions is quasi-cleavage as illustrated in Figure 4-23 (a). The characteristic feature of cleavage fracture, flat facets, is observed on these fracture surfaces. The flat facets are covered fully and partially by river markings and dimples on the fracture surface of the squeeze cast specimen. The river marking is the result of the crack

moving through the grain along a number of parallel planes, which forms a series of plateaus and connecting ledges. The dimples are caused by the localized microvoid coalescence. These features are an indication of the absorption of energy through local deformation. The entire fracture surface of the squeeze cast specimen in as-cast condition is characterized by the presence of deep dimples. The fractograph with higher magnification, Figure 4-23 (b), portrays dimples with extensive deformation marking along the walls of individual craters. A considerable amount of energy is consumed in the process of the formation of microvoids and microvoid-sheet, eventually leading to the creation of cracks. Thus, this type of fracture failure results from the coalescence of microvoids under the tensile stress.

However, the tensile fracture surface of the hybrid composites is quite different, in brittle manner. Much fewer dimples were found on the fracture surface of composite in Figure 4-24. Extensive matrix cracking and fibre cracking and debonding from matrix alloy were observed on the facture surface of the hybrid composites specimens, which leads to a premature failure at relatively low strains, but at high stress loads. Both of particle/ matrix and fibre/matrix interface debonding are also observed. Obviously, the localized damages, matrix cracking (arrow 1), interface debonding (arrow 2), fibre cracking (arrow 3), and particle cracking (arrow 4) as shown in Figure 4-25 (a-d) are the main reasons for the brittle fracture and, hence, the poor ductility of the composite material. The SEM observation on the fractured surfaces of the matrix alloy and composites are consistent with the obtained tensile properties given in the previous section.
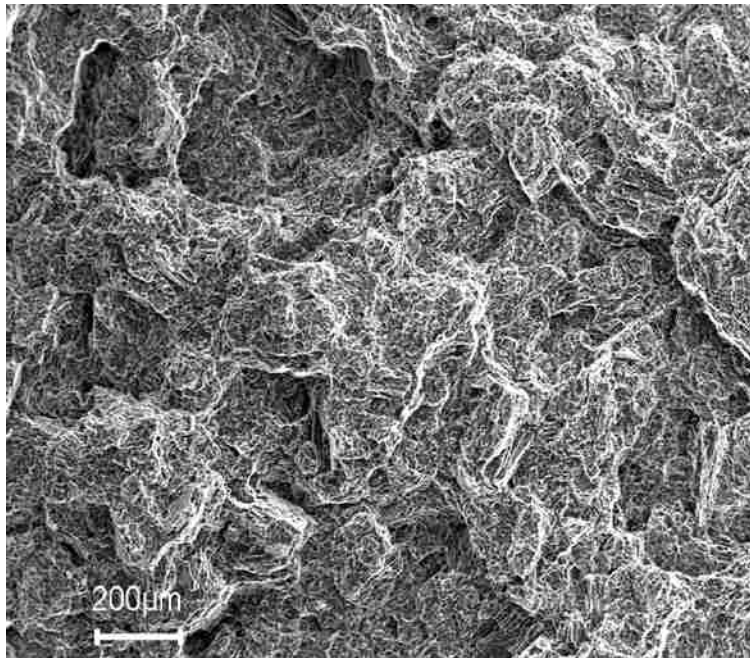
(a)
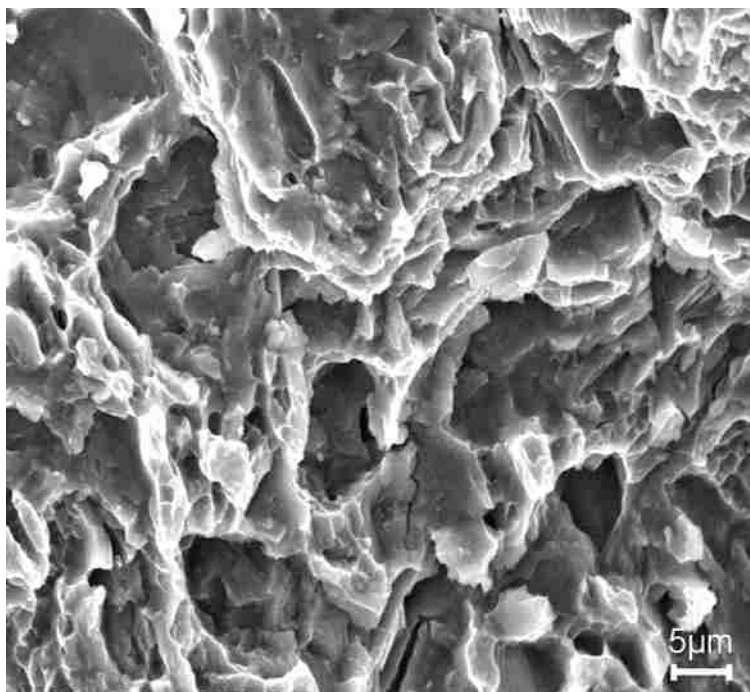
(b)

Figure 4-23 SEM fractographs of matrix AM60 alloy, (a) low magnification and (b) high magnification.
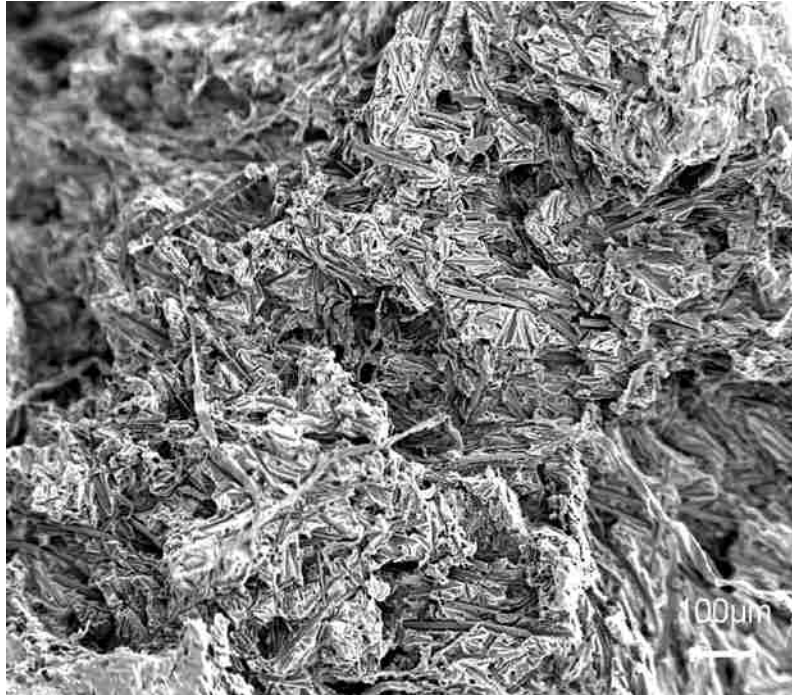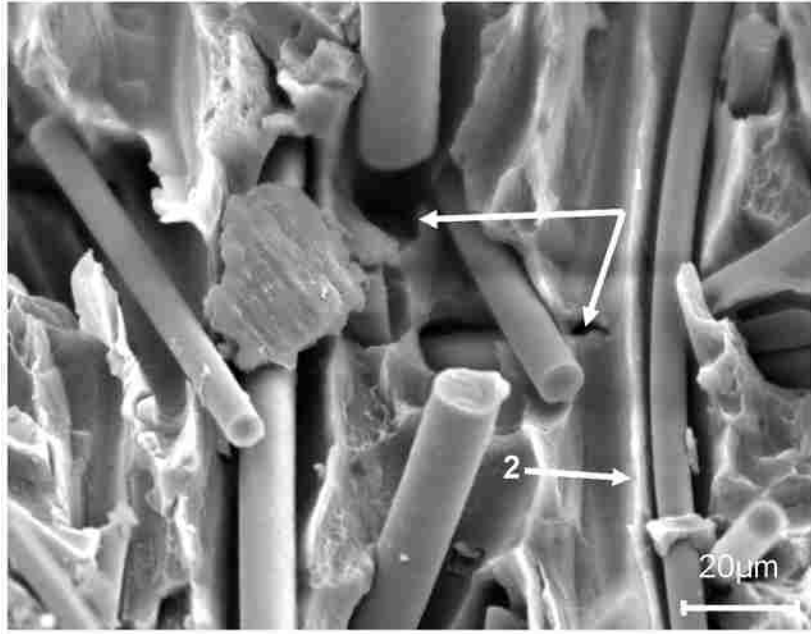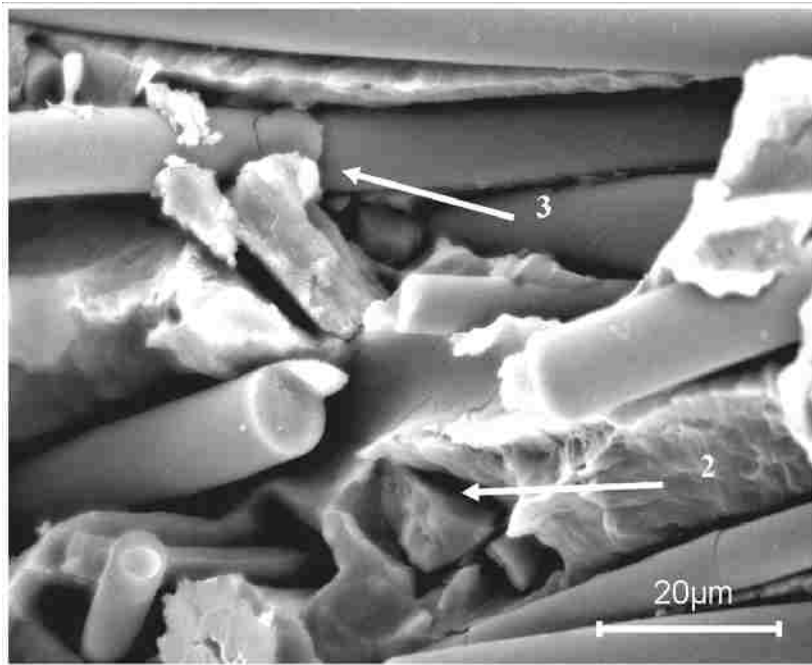
(a)
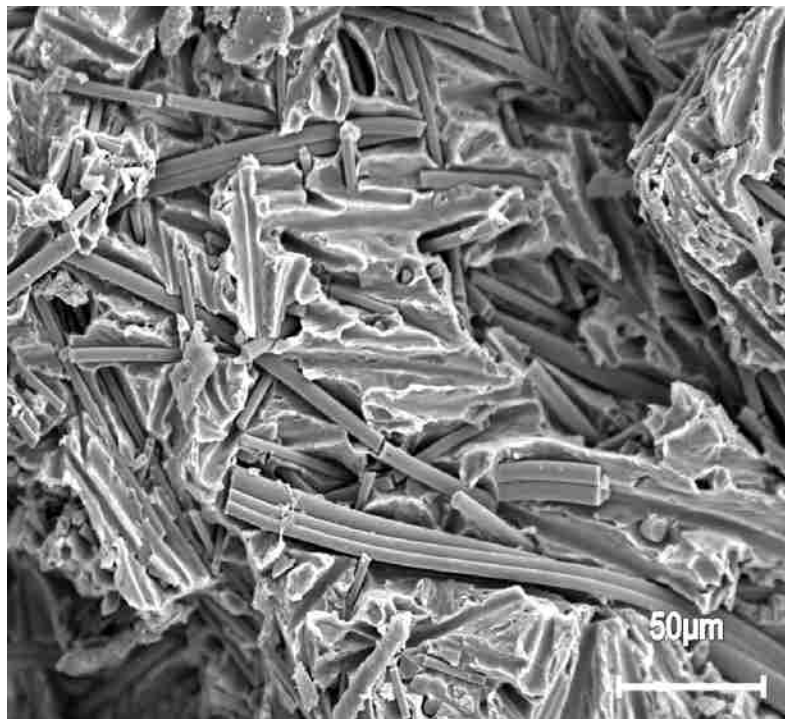
(b)

Figure 4-24 SEM fractogrpahs of hybrid composites, (a) low magnification and (b) high magnification.
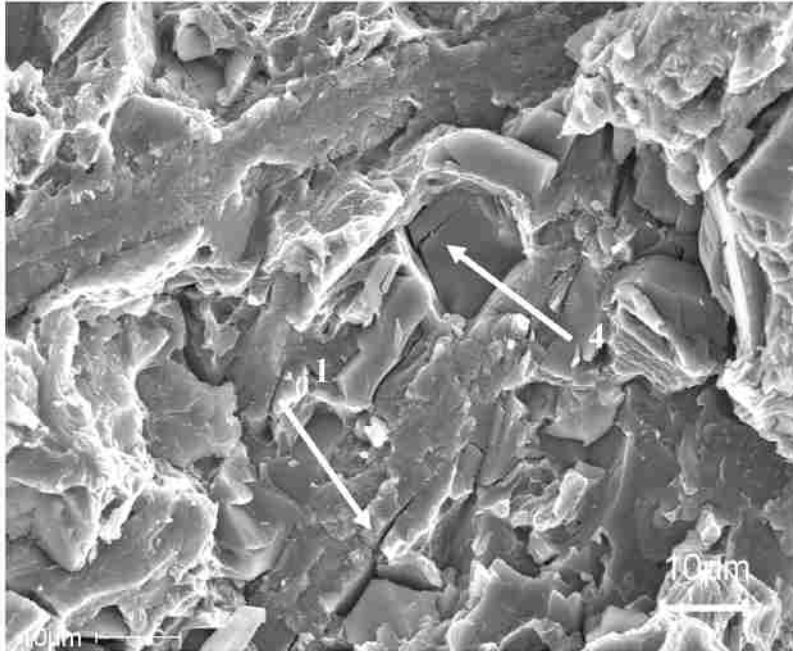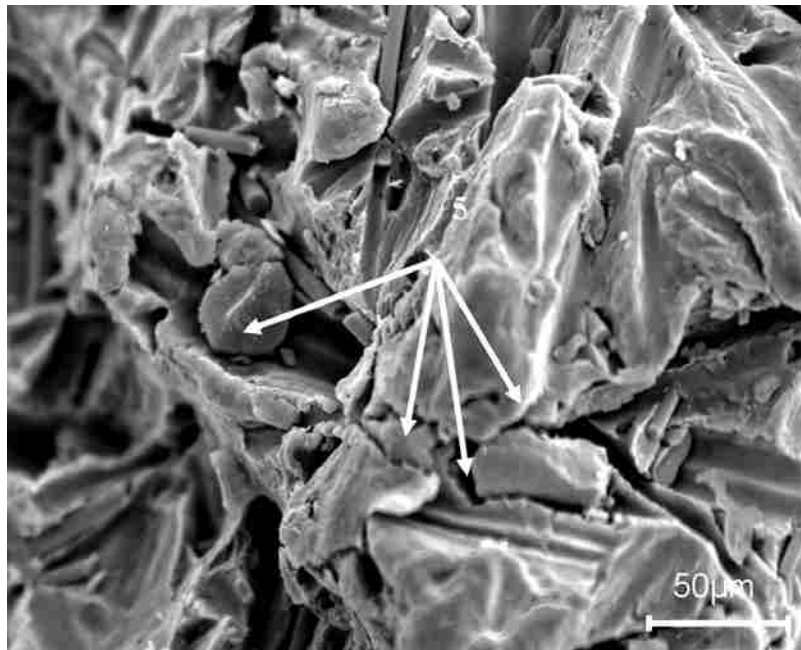
(a)

(b)

(c)

(d)

Figure 4-25 Localized damages hybrid composites, Arrow 1-matrix cracking, Arrow 2- interface debonding, Arrow 3-fibre cracking, Arrow 4-particle cracking, and Arrow 5- cracking going along the particle and matrix alloy.

It is mentioned early that the squeeze cast structure of AM60 and its hybrid composites is characterized by the α-Mg grains, eutectic phase $Mg_{17}Al_{12}$, and reinforcing particles and fibres. During plastic deformation, the slip behavior of each Mg grain is highly constrained by intragranular and intergranular particles and fibres, which are too strong to be deformed. For continuity of the hybrid composite under the external load, a strong internal stress must develop between reinforced particles and fibres and the matrix, which resists slip in the matrix to result in the strain-hardening. Consequently, localized damages, such as particles and fibres damage and cracking, matrix cracking, and interface debonding take place in the final stage of the tensile deformation. They are dominant in the fracture of the hybrid composites.

In addition the damaged microstructures underneath the fractured surfaces also presented in Figure 4-26 support the above interpretation.
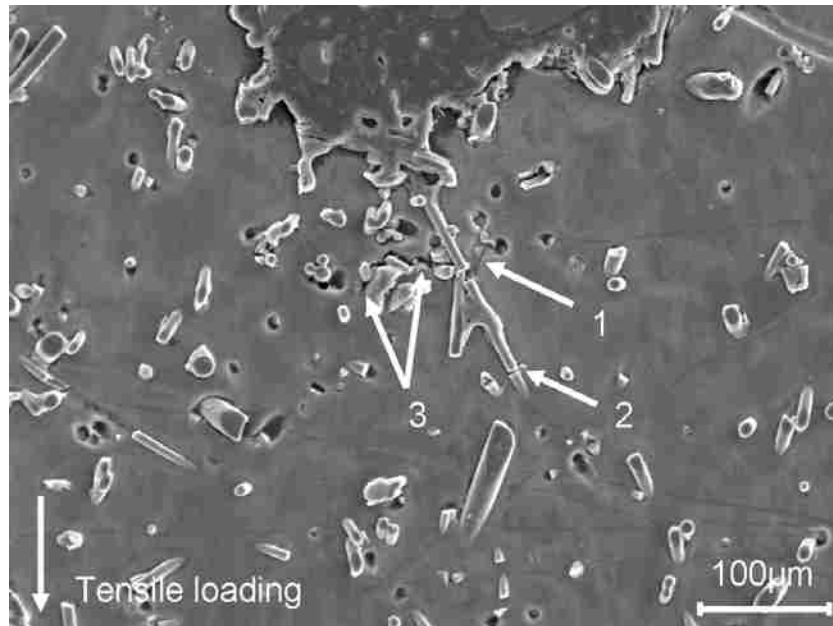

Figure 4-26 SEM fractographs showing the damaged microstructure underneath the fracture surfaces, Arrow 1-matrix cracking, Arrow 2- fibre cracking and Arrow 3-cracking going along the particle, fibre and matrix alloy.

Overall, the SEM observations of the fracture surfaces show a good agreement with the tensile behavior of the matrix alloy and its composites.

4.5 Summary

Hybrid composites are fabricated by adding two reinforcements into matrix materials so that the expected excellent properties can be achieved through the combined advantages of short fibres, and different size particles, which provide a high degree of design freedom. The preform-squeeze casting process was adopted to infiltrate the liquid Magnesium alloy into preform under an applied pressure. The results of preliminary microstructure analyses with both optical and scanning electron microscopy show that the ceramic reinforcement including both the particles and fibres are dispersed uniformly in the matrix alloy without agglomeration and cave. The property evaluation indicates that the hybrid reinforced composite has improved elastic modulus, tensile strengths and hardness in comparison to the matrix alloy. The observation of SEM fractographs indicates that the fracture mode of the composites is the evolution of localized damages, such as particles and fibres damage and cracking, matrix cracking, and interface debonding, which is consistent with the tensile results.

The observation of solidification process on the matrix alloy and its composites implies a significant refinement of the matrix grain structure. This implication is evidenced by both optical and SEM microstructural analyses, and the grain size measurement. The microstructural analysis suggests the occurrence of both particle capture and pushing during the solidification of the hybrid composites. The investigation of grain refinement mechanisms indicates that the effect of the heterogeneous nucleation of the primary magnesium phase on Al_2O_3 particulates, the heterogeneous nucleation of the eutectic phase on both Al_2O_3 particulates and fibres and the

restricted   growth of magnesium crystals should be responsible for the final formation of fine

grains in the hybrid composites.

CHAPTER 5

CONCLUSIONS

The conclusions drawn from this study are summarized as follows:

1. A preform-squeeze casting process has been developed and applied to effectively fabricate magnesium-based fibre and particle-reinforced hybrid composites. To minimize fibre crushes and fractures in a brittle manner under compression stresses, it is found that a gradual increase in applied pressures can effectively prevent the deformation of hybrid preform during squeeze casting.

2. The SEM observation on the microstructure reveals that in the prepared hybrid preform, the fibres form the solid supporting frame, in which the ceramic particles are homogeneously dispersed in the three-dimensional skeleton structure.The microstructure analysis of the composites indicates that both particles and fibres disperse uniformly in the matrix alloy without agglomeration, and fibres orientate randomly in the matrix.

3. The investigation of grain refinement mechanisms indicates the particles could be served as heterogeneous nucleation sites for the primary α-Mg phase, and both fibres and particles could become the heterogeneous nucleation substrate of the eutectic phase of the matrix alloy. For the hybrid composites, the fibre-influenced heat accumulating capability of the materials is one of the dominant factors controlling heat transfer during the solidification process. However, the particles indeed play main role for in the grain refinement during the solidification of the primary α-Mg in the hybrid composites.

4. The hybrid composite reinforced with 4vol% Al_2O_3 particles and 9vol% Al_2O_3 fibres exhibits improved tensile strengths over those of the matrix alloy. In particular, the yield strength (150MPa) of the hybrid composite is 88% higher than that of the matrix alloy. With almost no increase in density, the elastic modulus of the hybrid composite (59GPa) shows 40 % improvement over that of the matrix alloy (40GPa).

5. Compared to the ductile fracture of the matrix alloy, the SEM fractography reveals that the fracture of the hybrid composites is in brittle mode. The localized damages, i.e., reinforcement cracking, matrix cracking and interface debonding, should be responsible for the tensile fracture of the Mg-based hybrid composites.

CHAPTER 6

FUTURE WORK

Because the size of reinforcement for both particle and fibre has a significant influence on the engineering performance and microstructure development of composites, the future work for this study can be classified into the following research areas:

1. Development of a process for fabricating hybrid composites based on nano-sized particles and fibres;

2. Detailed studies on solidification and characterization of the hybrid composites reinforced with nano-sized particles and fibres;

3. Investigation in wear and corrosion behaviours of hybrid composites for potential engineering applications;

4. TEM investigation in the effect of microstructure such as slip and dislocation movement in matrix alloy on tensile behaviour of the hybrid composites; and

5. Development of thermal treatment schemas (T4 and T6), in which the tensile properties of the hybrid composites are optimized.

REFERENCES

[1] E. Warda Ⅱ, Light Metals Age Feb. (1989): 34.

[2] A. Luo, J. Renaud, I. Najatsygwa and J. Plourde, JOM July (1995): 28.

[3] B. Clow, Adv. Mater. Proc. Feb. / Oct. (1996): 33.

[4] M. Zhou, H. Hu, N. Li and J. Jo, Microstructure and tensile properties of squeeze cast magnesium alloy AM50, Journal of materials engineering and performance, (14), 2005, 539-545.

[5] M. Ozden and A. Luo, Patent, WO 96/25529.

[6] I. Polmer, "Light Alloys, 2nd" Published by Edward Arnold (1989): 169.

[7] F. Buch, J. Lietzau, B. Mordike, A. Pisch and R. Schmid, Mater. Sci. Engng. A 263 (1999): 1.

[8] "Magnesium Industry (Italy)," Dec. 2000, Vol. 1, No. 3, 22.

[9] A. Diwanji and I. Hall, J. Mater. Sci. 27 (1992) 2093.

[10] Y. Kagawa and E. Nakata, J. Mater. Lett. 11(3) (1992) 176.

[11] O. Ottinger, W. Schaff, C. Hausmann, T. Yne and R. F. Singer, in Proc. ICCM-11, Gold Coast, Austraila, ICCM-11, 1997, 804.

[12] R. Lee and W. Jones, J. Mater. Sci. 9 (1974): 469.

[13] Gibson, Sshby, Cellular solids, Cambridge University Press; 1997.

[14] A. Alamo and A. Banchik, J. Mater. Sci. 15 (1980) : 222.

[15] P. Frost, J. Kura, et al, Trans. AIME 188 (1950): 1277.

[16] A. Luo, Metall. Mater. Trans. A 26A (1995): 2445.

[17] R. Saravanan and M. Surappa, Mater. Sci. Engng. A 276 (2000): 108.

[18] B. Mikucki, W. Mercer and W. Green, Light Met. Age 48(5/6) (1990): 12.

[19] S. Lim and T. Choh, J. Jpn. Inst. Met. (Japan) 56(9) (1992) 1101.

[20] B. Inem and G. Pollard, DGM Information sgesell schaft M.B.H., Germany, 1992, 439.

[21] T. Wilksandj, F. King, DGM Information sgesell schaft M.B.H., Germany, 1992, 431.

[22] K. Wu, M. Zheng, C. Yao, S. Tatsuo, T. Hiroyasu, K. Akihiko and D. Li, J. Mater. Sci. Lett. (0261-8028) 18(16) (1999): 1301.

[23] K. Wu, M. Zhao, and J. Li, Scripta Materialia 35(4) (1996): 529.

[24] G. Chadwick and A. Bloyce, Magnesium Alloys and Their Applications, Garmisch-Partenkirchen, Germany, April 1992, DGM Informationsgesellschaft M.B.H., Germany, 1992, 93.

[25] H.Hu. Squeeze casting of Magnesium alloys and their composites, Journal of materials science, 33, 1998, 1579-1589

[26] J.Narciso, C.Garcia-cordovilla and E.Louis: Acta Materi.1997, 45, 5111-5118

[27] Y.Nishida, and G.Ohira, Modelling of Infiltration of Molten in Fibrous Preform by Centrifugal Force, Acta mater.Vol.47, 841-852, 1999

[28] J. Sekhar, Scripta Metall. 19 (1985) 1429.

[29] L. X. HU and E. D. WANG, Mater. Sci. Engng. A 278 (2000): 267.

[30] K. Soh, K. Euh , S. Lee and I. Park, Metall. Mater. Trans.A 29A (1998): 2543.

[31] M. Zarinejad, S. Firoozi, P. Abachi and K. Purazrang, "Canadian Institute of Mining, Metallurgy and Petroleum," (Metal/Ceramic Interactions, Canada, 2002). 191.

[32] J. Lo, and R. Santos, Magnesium matrix composites for elevated temperature applications, 2007 SAE World Congress, SAE, Detroit, MI, 2007-01-1028.

[33] Q. Zhang, and H. Hu, Processing and Characterization of Al-based Hybrid Composites, EPD 2009, TMS, 2009: 769-775.

[34] J. Idris and J. Tan, "Minerals, Metals and Materials Society/AIME" (Magnesium Technology, USA, 2000), 311.

[35] L. Lu, B. Chua and M. Lai, Comp. Struct. (UK), 47(1–4) (1999): 595.

[36] A. Yamazaki, J. Kaneko, and M. Sugmata, J. Jpn. Soc. Powder Powder Metall. (Japan) 48(10) (2001): 935.

[37] H. Hu, Grain Microstructure Evolution of Mg (AM50A)/SiCp Metal Matrix Composites, Journal of materials science, vol.39, No.8, 1998:1015-1022.

[38] S. Sundararajan, R. Mahadevan and E. Dwarakadasa, inTenth International Conference on Composite Materials. II. Metal Matrix Composites (Woodhead Publishing Limited, 1995): 831.

[39] A. Sato and R. Mehrabian, Metall. Trans. B 7B (3) (1976) 443.

[40] M. Zheng, K. Wu, H. Liang, S. Kamado and Y. Kojima, Mater. Lett. 57 (2002): 558.

[41] S. Hassan and M. Gupta, J. Alloys Comp. 335(1/2) (2002): 10.

[42] Idem, Mater, Res. Bul. 37(2) (2002): 377.

[43] R. Armstrong, I. Codd, R. Douthwaite and N. Petch, Phil. Mag. 7 (1962): 45.

[44] A. Luo, Scripta Metallurgica et Materialia (0956-716X) 31(9) (1994) 1253.

[45] Y. Cai, M. Tana, G. Shen and H. Su, Mater. Sci. Engng. A 282 (2000): 232.

[46] A. Luo (Woodhead Publishing Limited, UK, 1995): 287.

[47] F. Moll, K. Kainer andB. Mordike, "Magnesium Alloys and Their Applications," edited by B. L. Mordike and K. U. Kainer , Frankfurt, Werstoff information sgesell schaft, 1998.

[48] F. Moll, Dissertation Work, TU Clausthal, Germany (in German, 2000).

[49] P. Ghosh and S. Ray, J. Mater. Sci. 21 (1986): 1667.

[50] H. Hu and A. Luo, JOM (USA) 48(10) (1996) 47.

[51] X. Zhang, D. Zhang, R. Wu, Z. Zhu and C. Wang, Scripta Metallurgica (1359-6462) 37(11) (1997) 1631.

[52] P.Chen, Y.Sun, J.Jing, and Q.Lu, Chinese J.Nonferr.Met. (China) 12 (1997)140.

[53] B. Inem and G. Pollard, J. Mater. Sci. 28 (1993): 4427.

[54] J.Schroder, K.Kainera and B.Mordike, Developments in the science and technology of composites materials, ECCM 3, Bordeaux, France, 20-23 March 1989.

[55] M. Russell, D. Plane, J. Summerscales, P. Schulz and M. Papakyriacou, Mater. Sci. Techn. 18 (2002): 501.

[56] M. Zhao, M. Zhang, K. Wu, W. Peng and T. Lei, J. Mater. Sci. Lett. 22 (2003): 643.

[57] M. Svoboda, M. Pahutova, K. Kucharova, V. Skilenicka and T. Langdon, Mater. Sci. Engng. A 324 (2002): 151.

[58] Y. Li and T. Langdon, Metall. Mater. Trans. 30A (1999): 2059.

[59] V. Sklenicka, M. Pahutova, K. Kucharova, M. Svoboda and T. Langdon, Metall. Mater. Trans. A (USA) 33A (3A) (2002): 883.

[60] D.A.Porter, K.E.Eastering, Phase transformations in metals and alloy, Van Nosgtrand Reinhold Co, 1981.

[61] M. Yoo, Y. Kim, S. Ahn and N. Kim, Mater. Sci. Forum 419–422 (2003): 419.

[62] H. Wantanbe and T. Mukai, Scripta Mater. 42 (2000)

[63] D.R. Poirier, G.H.Geiger, Transport phenomena in Materials processing, A publication of the minerals, metals& materials society, USA, 1994.

[64] Magma soft database, Magma Foundry Technologies, Inc., Schaumburg, Illionois, USA, 2002.

[65] James A. Dicarlo, High temperature structural fibers- status and needs, NASA .Technical

memorandum 105174, May 1991

[66] Q. Jing, Solidification microstructures in a short fiber reinforced alloy composite containing different fiber fractions, China Foundry. Vol.3, No.1, Feb.2006

[67] W. Li, and H. Fan, Temperature effect on aging behavior of mullite / Al-4.0 Cu composites and its base alloy, Rare Metals, 27(2), 2003: 229-232.

[68] J. H. Hollomon, Tensile deformation, Transactions of the American Institute of Mining and Metallurgical Engineers, vol.162, 1945: 268-275.

VITA AUCTORIS

NAME: QIANG ZHANG

COUNTRY OF BIRTH: CHINA

DATE OF BIRTH: 1969

EDUCATION: Shannxi Institute of Mechanical Engineering, Xi'an, China

Department of Materials Science and Engineering

1987-1991, B.Sc.

University of Xi'an Technology, Xi'an, China

Department of Materials Science and Engineering

1991-1994, M.Sc.

University of Windsor, Windsor, On, Canada

Department of Mechanical, Automotive and Materials Engineering

2008-2009, M.Sc.